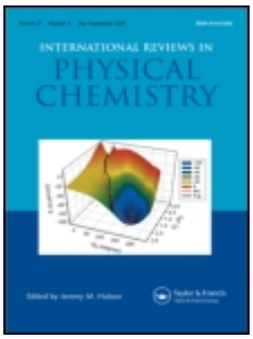

International Reviews in Physical Chemistry

ISSN: 0144-235x (Print) 1366-591X (Online) Journal homepage: www.tandfonline.com/journals/trpc20

Vibrational spectroscopy of the hydrogen bond: An ab initio quantum-chemical perspective

Janet E. Del Bene & Meredith J. T. Jordan

To cite this article: Janet E. Del Bene & Meredith J. T. Jordan (1999) Vibrational spectroscopy of the hydrogen bond: An ab initio quantum-chemical perspective, International Reviews in Physical Chemistry, 18:1, 119-162, DOI: 10.1080/014423599230026

To link to this article: https://doi.org/10.1080/014423599230026

Published online: 26 Nov 2010.

INTERNATIONAL REVIEWS IN PHYSICAL CHEMISTRY, 1999, VOL. 18, NO. 1, 119–162

Vibrational spectroscopy of the hydrogen bond: an *ab initio* quantum-chemical perspective

JANET E. DEL BENE

Department of Chemistry, Youngstown State University, Youngstown, Ohio 44555-3663, USA

and MEREDITH J. T. JORDAN

Department of Chemistry, University of Sydney, Sydney, New South Wales, 2006, Australia

The hydrogen bond has long been recognized as an important type of intermolecular interaction. Its infrared (IR) spectroscopic signature is the shift to lower frequency and the increase in intensity of the A–H stretching band upon formation of the A–H···B hydrogen bond. *Ab initio* calculations carried out with an appropriate wavefunction model and basis set, and using the harmonic approximation, can reasonably reproduce the shift of the A–H stretching band upon hydrogen bonding, if the equilibrium structure exists in a relatively deep potential well on the surface, so that both the $v = 0$ and the $v = 1$ vibrational states of the proton-stretching mode are confined within this well. However, if the equilibrium structure is found in a region of the surface which is broad and relatively flat, or if a second region of the surface can be accessed in either the $v = 0$ or the $v = 1$ vibrational state of the proton-stretching mode, then the harmonic approximation fails to describe the anharmonicity inherent in the surface. For such complexes, experimental gas-phase structures and experimental IR spectra obtained in low-temperature rare-gas matrices may give conflicting descriptions of the hydrogen bond, and discrepancies will exist between experimental and computed harmonic IR spectra. Anharmonic frequencies for both fundamental and combination bands are needed to understand and reproduce qualitatively the most important features of the experimental spectra. In this article, an overview of the calculation of anharmonic frequencies is presented, and results of one- and two-dimensional anharmonic treatments of vibration are reported for a variety of hydrogen-bonded complexes. Computed frequencies are compared with experimental gas-phase frequencies when these are available, and with experimental frequencies obtained in low-temperature rare-gas matrices.

Contents

International Reviews in Physical Chemistry ISSN 0144-235X print/ISSN 1366-591X online © 1999 Taylor & Francis Ltd
http://www.tandf.co.uk/JNLS/rpc.htm http://www.taylorandfrancis.com/JNLS/rpc.htm

1. Introduction

The hydrogen bond has long been recognized as an important type of intermolecular interaction, which dramatically influences the properties of chemical and biochemical systems (Pimentel and McClellan 1960). Long before the hydrogen bond was recognized and given a name, it was observed experimentally through measurements of anomalous physical and thermodynamic properties. One property traditionally associated with the presence of a hydrogen bond is the shift in the infrared (IR) spectrum of the A–H stretching band upon formation of the A–H ··· B hydrogen bond. This shift and the increase in intensity of the A–H stretching band provide experimental evidence for the existence of a hydrogen bond and are so characteristic that they have become its spectroscopic signature.

Formation of a hydrogen-bonded complex converts three degrees of translational freedom and three degrees of rotational freedom (assuming nonlinear molecules) into six new intermolecular vibrational modes, including the intermolecular stretching mode (the 'dimer' stretch), and the hydrogen bond bending mode. The intermolecular modes usually have low frequencies, often below 400 cm^{-1}. In a typical complex, the intramolecular modes are only slightly perturbed by hydrogen bond formation. The exception, of course, is the shift of the A–H proton-stretching mode to lower frequency in a complex containing an A–H ··· B hydrogen bond. It is the characterization of this mode which will be the major focus of this article.

Ab initio theoretical studies of the hydrogen bond began to appear in the late 1960s and early 1970s (Morokuma and Pedersen 1968, Kollman and Allen 1969, 1972, Morokuma and Winick 1970, Del Bene and Pople 1970, Hankins *et al.* 1970). These early studies were carried out in the context of single-determinant Hartree–Fock theory using small basis sets. Geometry optimization to determine the structure of a hydrogen-bonded complex was usually done by freezing monomer geometries, that is the geometries of the proton donor and proton acceptor species, and optimizing only the intermolecular coordinates. The optimization scheme was essentially done by hand, varying each intermolecular coordinate in turn cyclically and independently, until changes in these coordinates were less than some predefined threshold. At convergence, the binding energy of the complex was computed as the difference between the total energy of the complex and the sum of the energies of the respective monomers. IR spectral data were not computed.

A major breakthrough in *ab initio* studies of isolated molecules and hydrogen-bonded complexes occurred when techniques were developed for evaluating first and second derivatives of the energy with respect to the nuclear coordinates. These derivatives were first evaluated numerically, and later analytically (Pople *et al.* 1979, Schlegel 1982, 1994, Schlegel *et al.* 1984, Fogarasi and Pulay 1984, Pulay 1987, Dykstra *et al.* 1990, Bartlett *et al.* 1991, Gauss and Cremer, 1992) and the algorithms for doing this have been incorporated into *ab initio* software packages. As a result, automated full geometry optimizations are now routine. The same techniques can be used to compute vibrational spectra within the harmonic approximation.

2. Calculation of harmonic vibrational frequencies

The equilibrium structure of a hydrogen-bonded complex lies in a global minimum on the potential energy surface. This minimum is probed experimentally through vibrational IR spectroscopy and can be described theoretically by *ab initio* calculations. These calculations are usually carried out in the harmonic approximation, which means that the surface in the vicinity of the energy minimum is fitted by functions containing only a quadratic dependence of the energy on the nuclear coordinates, higher terms in the Taylor expansion being neglected. The vibrational problem is routinely solved using the **GF** matrix formulation (Wilson *et al.* 1955). The vibrational wavefunction can be expressed as a direct product of harmonic oscillator functions, one for each normal coordinate. Normal coordinates are linear combinations of mass-weighted Cartesian displacement coordinates, and this often complicates their description in terms of simple stretches and bends. However, in a hydrogen-bonded complex the proton-stretching mode is often essentially a pure A–H stretch, perturbed by the presence of the A–H···B hydrogen bond, and occurring at a lower frequency than the monomer A–H stretch. The total vibrational energy of the system is simply the sum of the vibrational energies of the harmonic oscillators.

In the harmonic approximation, the total energy of the optimized structure of a molecule or complex consisting of N atoms can be written as (Hehre *et al.* 1986)

$$E = T + V = \frac{1}{2}\sum_{i=1}^{3N} \dot{q}_i^2 + V_{\mathrm{eq}} + \sum_{i=1}^{3N} \frac{\partial V}{\partial q_i} + \frac{1}{2}\sum_{i=1}^{3N}\sum_{j=1}^{3N} \left(\frac{\partial^2 V}{\partial q_i\, \partial q_j}\right)_{\mathrm{eq}} q_i\, q_j,$$

where mass-weighted Cartesian displacements q_i are defined in terms of the locations x_i of the nuclei relative to their equilibrium positions $x_{i,\,\mathrm{eq}}$ and their masses M_i:

$$q_i = M_i^{1/2}(x_i - x_{i,\,\mathrm{eq}}),$$

V_{eq} is the potential energy at the equilibrium nuclear configuration, and the expansion has been truncated at second order. For such a system, the classical-mechanical equations of motion are

$$\ddot{q}_j = -\sum_{i=1}^{3N} f_{ij}\, q_i, \quad j = 1, 2, \cdots, 3N,$$

where f_{ij} are the quadratic force constants, which are the second derivatives of the potential energy with respect to mass-weighted Cartesian displacements, evaluated at the equilibrium nuclear configuration:

$$f_{ij} = \left(\frac{\partial^2 V}{\partial q_i\, \partial q_j}\right)_{eq}.$$

Solution of the equations of motion yields a set of $3N - 6$ ($3N - 5$ for linear systems) normal-mode vibrational frequencies.

In the Taylor series expansion of the potential energy, the first derivative term of the energy with respect to the nuclear coordinates is zero, since the equilibrium structure is a stationary point on the potential energy surface. As a consequence, the calculation of the vibrational spectrum of a molecule or complex must be performed at the same level of theory (wavefunction model and basis set) used for geometry optimization. The computed harmonic spectrum depends on the nature of the equilibrium structure, and therefore on the method used to compute this structure. This methodological dependence will be discussed below.

In the harmonic approximation, terms in the Taylor series expansion of the potential higher than second order are neglected. There are several important consequences of this approximation.

(1) The potential energy surface near the minimum is described by a set of orthogonal parabolic curves, one for each normal coordinate.
(2) The energy levels for each normal mode are equally spaced, with the vibrational energies given as

$$E_i = \left(n + \frac{1}{2}\right) hc\omega_i \text{ for } n = 0, 1, 2, \ldots,$$

with ω_i the vibrational frequency (expressed in reciprocal centimetres) of a normal mode.
(3) The computed vibrational frequencies are usually too high relative to experiment, independent of the level of theory used for the calculation. This is due to the anharmonicity of the potential energy surface, described by the higher-order terms in the Taylor expansion which are neglected in the harmonic approximation.
(4) The selection rule for vibrational excitation is $\Delta n = \pm 1$. The frequency of the $n = 0 \rightarrow n = 1$ vibrational excitation is referred to as the fundamental frequency. Within this approximation there are no overtone or combination bands in the spectrum.

(5) Intensities are computed from the derivatives of the dipole moment vector with respect to the normal coordinates (Yamaguchi *et al.* 1986). The intensity A_i for absorption for a particular normal mode is

$$A_i = \frac{N\pi}{3c^2}\left(\frac{\partial\mu}{\partial q_i}\right)^2,$$

where N is Avogadro's constant, c is the speed of light and q_i is the normal coordinate of the ith mode.

How well does a parabolic description of a normal mode describe a minimum on a potential energy surface along this coordinate? If the minimum is deep and the displacement from equilibrium during the vibration is small, then approximating the minimum by a parabola should be reasonable. Harmonic frequencies computed for a set of diatomic molecules at the Hartree–Fock level with the 6-31G(d) basis set were found to be about 11% too large (Hehre *et al.* 1986). The errors in the computed frequencies arise from two sources: firstly the steepness of the Hartree–Fock potentials and secondly the neglect of anharmonicity. Potentials computed with electron correlation effects included are softer, so that the frequencies for the same set of molecules obtained at second-order Møller–Plesset theory (MP2/6-31G(d)) (Pople *et al.* 1976, Bartlett and Silver 1975) are improved, overestimating experimental values by 4.6% (Hehre *et al.* 1986). Further improvement can be obtained by using higher levels of correlation, such as coupled-cluster methods (Purvis and Bartlett 1982, Urban *et al.* 1985, Raghavachari *et al.* 1989, Bartlett 1989, Bartlett *et al.* 1990, Watts *et al.* 1993) with larger basis sets. However, the errors which remain in these treatments are inherent to the harmonic approximation and its neglect of the anharmonicity of the potential energy surface. Can the harmonic approximation be expected to describe adequately the A–H stretching frequency in a hydrogen-bonded complex? Or can the harmonic approximation at least give reliable frequency shifts upon hydrogen bonding? These questions will be addressed in the following sections.

3. Methodological dependence of structures and harmonic spectra of hydrogen-bonded complexes

The computed harmonic vibrational spectrum of a complex is dependent on the description of the potential energy surface, in terms of both the nature of the equilibrium structure, and the depth and curvature of the potential well along each normal coordinate. Two structural features strongly influence the computed IR spectrum, namely the intermolecular (hydrogen bond) A–B distance, and the change in the A–H bond length relative to the A–H distance in the isolated proton-donor molecule. Since there is a methodological dependence of the computed structure of a hydrogen-bonded complex (Del Bene *et al.* 1995, Del Bene and Shavitt 1997), it is important to identify at which levels of theory reliable structures can be obtained. These structures can be judged by applying two criteria. The first is convergence with respect to further extension of the methodology. This means that the computed structure will not significantly change when recomputed using a more sophisticated wavefunction or a larger basis set. The second criterion is comparison of converged structures with reliable experimental data. Applying these criteria makes it possible to identify that level of theory required to give reliable structures at minimum computational expense.

Comparison of computed and experimental distances must be done with care. The

Table 1. Water dimer intermolecular distance R_e and electronic binding energy ΔE_e at various levels of theory. DZP, double zeta plus polarization; VDZ, explained in the text; QCISD, quadratic configuration interaction with single and double excitations; CCSD, coupled cluster with single and double excitations; CCSD(T), coupled cluster with single and double excitations with perturbative triples; TZ2P, triple zeta plus double polarization. Hartree–Fock (HF), Møller–Plesset second order (MP2) and configuration interaction with single and double excitations (CISD) results with basis sets derived from 6-31G and 6-311G are taken from the work of Frisch *et al.* (1986). The binding energies were computed at the same level of theory used for structure optimization.

Method	Basis set	R_e (Å)	ΔE_e (kcal^{-1} mol^{-1})
HF	STO-3G	2.740	−5.9
	3-21G	2.797	−11.0
	6-31G(d)	2.971	−5.6
	6-31G(d, p)	2.980	−5.5
	DZP	2.986	−5.0
	6-31 +G(d)	2.964	−5.4
	6-31 ++G(d)	2.959	−5.4
	6-31 +G(d, p)	2.988	−5.0
	6-31 ++G(d, p)	2.987	−5.0
	6-311 +G(d, p)	2.999	−4.8
	6-311 ++G(2d, 2p)	3.035	−4.1
	11 +7 +(2d, 2p)	3.033	−3.9
	6-311 ++G(3df, 3pd)	3.026	−4.0
MP2	3-21G	2.802	−12.7
	6-31G(d)	2.913	−7.4
	6-31G(d, p)	2.910	−7.1
	DZP	2.909	−6.3
	6-31 +G(d)	2.901	−7.1
	6-31 ++G(d)	2.895	−7.2
	6-31 +G(d, p)	2.914	−6.5
	6-311 +G(d, p)	2.908	−6.1
	6-311 ++G(d, p)	2.910	−6.1
	6-311 ++G(2d, 2p)	2.911	−5.4
	cc-pVDZ	2.908	−7.5
	aug´-cc-pVDZ	2.923	−5.2
	aug´-cc-pVTZ	2.909	−5.0
CISD	6-31G(d)	2.937	
	6-31 +G(d)	2.920	
QCISD	6-31 +G(d, p)	2.939	−6.0
	aug´-cc-pVDZ	2.954	−4.9
CCSD	aug´-cc-pVDZ	2.953	−4.9
CCSD(T)	DZP	2.922	−6.1[a]
	TZ2P	2.914	−5.4[a]
	aug´-cc-pVDZ	2.948	−5.1

[a] From Kim *et al.* (1995).

intermolecular distance measured experimentally is the average distance R_0 in the ground vibrational state. What is computed is the intermolecular distance R_e at the bottom of the potential well. The methodological dependence of the computed intermolecular distance is illustrated by the O–O distances in the water dimer, which are reported in table 1. These data show significant variation, with R_e ranging from 2.740 Å at the single-determinant Hartree–Fock level with the minimal STO-3G basis set, to 3.035 Å at Hartree–Fock with the 6-311 ++G(2d, 2p) basis set. The

Table 2. The intermolecular O–O distance in the water dimer obtained from high-level *ab initio* calculations (Xantheas and Dunning 1993, 1998, Feller *et al.* 1994): MP4, Møller–Plesset fourth-order.

	O–O distance (Å)						
Basis set	HF	MP2(fc)	MP2(fu)	CCSD	CCSD(T)	MP4(fc)	MP4(fu)
aug-cc-pVDZ	3.030	2.916	2.911	2.944	2.925	2.921	2.917
aug-cc-pVTZ	3.039	2.907	2.889	2.933	2.914	2.912	2.892
aug-cc-pVQZ´	3.037	2.907		2.932	2.913	2.912	
aug-cc-pVQZ	3.036	2.903					
aug-cc-pV5Z		2.905					

experimental O–O distance R_0 in the water dimer is 2.976 Å. Corrected for anharmonicity, the intermolecular distance R_e is estimated to be 2.946 Å (Dyke and Muenter 1973, Dyke *et al.* 1977, Odutola *et al.* 1979). Analysis of the data in table 1 shows that water dimer structures optimized at the Hartree–Fock level with all the augmented split-valence basis sets (i.e. all basis sets except STO-3G and 3-21G) have O–O distances that are too large. At the Hartree–Fock level the best agreement between theory and experiment is obtained at HF/6-311 ++G(d) with R = 2.959 Å. Unfortunately, this is not a converged Hartree–Fock value, since further expansion of the basis sets leads to poorer results. Including electron correlation effects reduces the computed O–O distance and its variation with basis set. At the MP2 level the intermolecular O–O distance appears to be underestimated by 0.023–0.051 Å relative to experiment.

Xantheas and Dunning (1993, 1998) have undertaken a very systematic and comprehensive study of the structure of the water dimer using various wavefunction models and Dunning's augmented correlation-consistent split-valence basis sets aug-cc-pVXZ, where X = D for double, T for triple, Q for quadruple and 5 for quintuple split (Dunning 1989, Kendall *et al.* 1992, Woon and Dunning 1993). These basis sets are ideally suited to convergence studies, since they have been constructed very systematically, based on calculations that included electron correlation effects. The intermolecular O–O distance in the water dimer computed with these basis sets at Hartree–Fock and different correlation levels are reported in table 2. At the Hartree–Fock level, the O–O distance in the water dimer is predicted to be 3.03 Å, significantly longer than the experimental distance. Calculations including electron correlation effects yield significantly shorter O–O distances. At correlated levels, increasing the basis set from aug-cc-pVDZ to aug-cc-pVTZ leads to small changes of 0.01 or 0.02 Å in the O–O distance. Further extension of the basis set has essentially no effect on the computed distance. The most extensive electron correlation treatment (CCSD(T) with the aug-cc-pVQZ´ basis set, where aug-cc-pVQZ´ is aug-cc-pVQZ without f functions on hydrogen atoms) leads to a computed intermolecular distance of 2.913 Å. Thus, the computed distances appear to converge to about 2.91 Å, with all the calculated distances being within 0.02 Å of this value. This value is significantly shorter than the estimated experimental intermolecular O–O distance (R_e = 2.946 Å). In $(H_2O)_2$ the O–O distance corresponds to a loosely bound mode, and vibrational averaging in the ground state may influence its length. Thus, the discrepancy between theory and experiment may be a manifestation of the anharmonicity in the intermolecular potential along this coordinate (see below).

The levels of structure optimization carried out by Xantheas and Dunning for the water dimer are computationally demanding and not feasible for routine studies of hydrogen-bonded complexes. Is there a lower level of theory which can consistently predict reasonable intermolecular distances and vibrational frequency shifts, and which can be applied routinely to larger 1:1 complexes? Table 3 presents computed intermolecular distances for a set of nine complexes for which experimental data are available. These calculations were carried out at Hartree–Fock and at the correlated MP2 level with two different basis sets, 6–31G(d) and 6–31 +G(d,p) (Hehre *et al.* 1972, Hariharan and Pople 1973, Spitznagel *et al.* 1982, Clark *et al.* 1983). The first basis set is a split-valence basis set with a set of d polarization functions on non-hydrogen atoms, a basis often used in studies of the structures and vibrational spectra of isolated monomers. The second basis is slightly larger, with first polarization functions on all atoms, and diffuse functions on non-hydrogen atoms. Diffuse functions are required to better describe the non-bonded electrons on B in the A–H···B hydrogen bond, and have important structural and energetic effects, as evident from tables 1 and 3. Several generalizations relating to intermolecular distances can be made from the data of table 3.

(1) Intermolecular distances computed at the Hartree–Fock level can be significantly different from experimental distances. Hartree–Fock distances are usually too long, often by more than 0.1 Å. The overestimation of the intermolecular distance in hydrogen-bonded complexes has severe consequences relative to the nature of the intermolecular hydrogen bonding surface. In particular, at the longer distances, double minima may appear in the curve for proton transfer. These double minima disappear at correlated levels of theory (Latajka *et al.* 1984, 1987, 1992, Del Bene 1998).
(2) The equilibrium HF/6-31G(d) and MP2/6-31G(d) structures of $(HF)_2$ are cyclic, in contrast with the open structure found experimentally and computed at higher levels of theory.
(3) In contrast with the water dimer where distances computed at MP2 with various augmented split-valence basis sets are similar, intermolecular distances computed at MP2/6-31G(d) and MP2/6-31 +G(d,p) may be different. When significant differences are found, the MP2/6-31 +G(d,p) distances are in better agreement with experimental data.

The weight of evidence suggests that Hartree–Fock calculations are not appropriate if reliable structures and potential energy surfaces for hydrogen-bonded systems are needed. The inclusion of electron correlation effects, at least at the level of MP2, is absolutely essential. It also appears that diffuse functions must be included in the basis set, so that MP2/6-31G +G(d,p) appears to be the minimum level of theory required for reliability. The data in table 3 suggest that, at this level, computed intermolecular distances agree with experimental distances to about 0.03 Å. Whether this is acceptable agreement will depend upon the particular application.

Computed harmonic and experimental frequency shifts of the A–H stretching band are also reported in table 3. Hartree–Fock frequency shifts computed with a given basis set are smaller than MP2 shifts computed with that same basis set and are usually too small relative to experimental shifts. As noted above, the steepness of Hartree–Fock potentials leads to underestimation of the lengthening of the A–H bond and the shift of the A–H stretching frequency. The softer MP2 potentials allow for a greater increase in the A–H bond and decrease in the A–H stretching frequency. For

Table 3. Intermolecular distances R and A–H vibrational frequency shifts δν in hydrogen-bonded complexes. Data for complexes of HF and HCl with HCN and CH_3CN were taken from Del Bene (1992) and MP2/6-31 +G(d, p) data for other complexes from Del Bene *et al.* (1995).

Complex	HF/ 6-31G(d)	HF/ 6-31 +G(d, p)	MP2/ 6-31G(d)	MP2/ 6-31 +G(d, p)	Experiment[a]
FH···NCH					
R (Å)	2.923	2.900	2.875	2.808	2.805[b]
$\delta\nu$ (cm^{-1})	106	176	119	262	245 (v)[c]
FH···$NCCH_3$					
R (Å)	2.878	2.850	2.835	2.758	
$\delta\nu$ (cm^{-1})	146	234	162	343	334 (v)[c, d]
ClH···NCH					
R (Å)	3.498	3.522	3.380	3.376	3.402[e]
$\delta\nu$ (cm^{-1})	73	68	126	113	79 (v)[f]
ClH···$NCCH_3$					
R (Å)	3.434	3.462	3.324	3.316	3.291[e]
$\delta\nu$ (cm^{-1})	110	103	173	167	155 (v)[g]
FH···CO					
R (Å)	3.145	3.198	3.080	3.062	3.047[h]
$\delta\nu$ (cm^{-1})	37	75	55	134	117 (v)[i, j]
ClH···OH_2					
R (Å)	3.242	3.288	3.152	3.185	3.215[k]
$\delta\nu$ (cm^{-1})	163	121	276	177	207 (Ar)[f]
ClH···ClH					
R (Å)	4.132	4.139	3.913	3.868	
$\delta\nu$ (cm^{-1})	13	14	28	32	53 (Ar)[f]
FH···FH					
R (Å)	2.596[l]	2.811	2.535[l]	2.777	2.79[m]
					2.72 ± 0.03[n]
$\delta\nu$ (cm^{-1})		89		116	93 (v)[o]
HOH···OH_2					
R (Å)	2.972	2.989	2.914	2.914	2.946[p]
$\delta\nu$ (cm^{-1})	42	50	67	79	64 (Ar)[q]

[a] Experimental vibrational data are shifts to lower frequencies from either vapour (v) or argon matrix (Ar) data.
[b] From Legon and Millen (1986).
[c] From Woodford *et al.* (1986, 1987a,b).
[d] From Legon *et al.* (1987).
[e] From Legon and Millen (1988).
[f] From Barnes (1983).
[g] From Ballard and Henderson (1991).
[h] From Legon *et al.* (1981).
[i] From Kyro *et al.* (1983).
[j] From Jucks and Miller (1987).
[k] From Legon and Millen (1992).
[l] The computed structure is cyclic with a short F–F distance.
[m] From Dyke *et al.* (1969).
[n] From Quack and Suhm (1991).
[o] From Pine and Lafferty (1983).
[p] From Dyke and Muenter (1973); Dyke *et al.* (1977) and Odutola *et al.* (1979).
[q] From Engdahl and Nelander (1989).

the seven complexes listed in table 3 for which vapour-phase experimental data are available, the computed A–H frequency shifts at MP2/6-31 +G(d,p) overestimate the experimental data, with the largest difference of 33 cm^{-1} occurring for ClH···NCH. When the experimental data are taken from argon matrix measurements, the computed MP2/6-31 +G(d,p) shifts for $ClH\cdots OH_2$ and $(HCl)_2$ are too small by 30 and 21 cm^{-1} respectively. Overall, however, the agreement is reasonable, and MP2/6-31 +G(d,p) has been recommended as the minimum level of theory required for computing A–H frequency shifts in 1:1 hydrogen-bonded complexes (Del Bene and Shavitt 1997). However, there are two observations that can be made at this point, both of which will be discussed in detail below.

(1) All the complexes in table 3 have traditional hydrogen bonds.
(2) The argon matrix can have an effect on the experimental IR spectrum.

4. Hydrogen bond type and shifts in harmonic vibrational frequencies

The A–H···B hydrogen bond between a pair of neutral molecules is a traditional hydrogen bond if the A–H covalent bond remains essentially intact in the complex. However, proton transfer may occur, giving rise to the hydrogen-bonded $A^-\cdots{}^+H{-}B$ ion pair. In principle there is nothing to limit the hydrogen bond to one of these two extremes. It was suggested over two decades ago that quasisymmetrical or proton-shared A···H···B hydrogen bonds may exist in certain complexes formed in low-temperature matrices or in the gas phase. The range of hydrogen bond types has been investigated recently in a systematic *ab initio* study of three series of hydrogen-bonded complexes formed between the hydrogen halides HX (X = F, Cl or Br) and a set of 4-substituted pyridines (4-R-pyridine) (Del Bene *et al.* 1996). Table 4 reports MP2/6-31 +G(d,p) structural and spectral data for the complexes with HCl, and figure 1 shows the computed spectra of the HCl:4-R-pyridine complexes. The listing of the substituted pyridines in table 4 and figure 1 is in the order of increasing proton affinity of the substituted pyridine.

The HCl:4-R-pyridine complexes with R = CN, F, Cl, H, CH_3 or NH_2 are complexes with traditional linear Cl–H···N hydrogen bonds. These complexes have intermolecular distances that range from 3.105 Å in HCl:4-CN-pyridine, the complex with the weakest hydrogen bond, to 3.002 Å in HCl:4-NH_2-pyridine, which has the strongest bond. The Cl–H distance in each complex is greater than the monomer distance of 1.270 Å and increases with increasing hydrogen bond strength and decreasing intermolecular distance. Figure 1 shows that these complexes exhibit a single strong perturbed H–Cl stretching band in the IR spectrum. The computed intensities of this band are about two orders of magnitude greater than the intensity of the monomeric H–Cl stretch. Figure 1 also shows the correlation between the frequency shift of the Cl–H stretching band and increasing binding energy of the complex.

In contrast with the first six complexes in this series which have traditional hydrogen bonds, the complexes HCl:4-Li-pyridine and HCl:4-Na-pyridine have proton-shared Cl···H···N hydrogen bonds. These are characterized by short Cl–N distances of 2.912 and 2.826 Å respectively and long H–Cl distances of 1.632 and 1.670 Å respectively. As the structures of these complexes change, so do their computed vibrational spectra. In contrast with the single strong proton-stretching band predicted for complexes with traditional hydrogen bonds, the complexes with

Table 4. Selected computed properties of ClH:4-R-pyridine complexes

R	Proton affinity[a, b] (kcal mol^{-1})	ΔE_e[c] (kcal mol^{-1})	ν(HCl) (cm^{-1})	A (HCl) (km mol^{-1})	R (Cl—H) (Å)	R (N—H) (Å)	R (Cl—N) (Å)
CN	210.4 (210.3)	9.2	2524	2315	1.309	1.796	3.105
F	217.0 (216.6)	10.0	2434	2458	1.316	1.759	3.075
Cl	218.4 (217.8)	10.0	2428	2658	1.316	1.758	3.074
H	220.0 (220.8)	10.7	2324	2844	1.323	1.721	3.044
CH_3	225.8 (225.2)	11.1	2271	3211	1.327	1.703	3.030
NH_2	233.5 (230)	11.7	2156	3665	1.336	1.667	3.002
			ν(HB st) (cm^{-1})	A (HB st) (km mol^{-1})			
Li	246.6	14.5	1296	3769	1.632	1.280	2.912
			877	1929			
			601	1501			
Na	251.3	15.7	1465	4928	1.670	1.156	2.826
			935	1291			
			599	539			
			ν(NH) (cm^{-1})	A (NH) (km mol^{-1})			
S^-	323.2	32.7	2636	5530	1.889	1.068	2.958
O^-	333.3	39.0	2826	3799	1.939	1.057	2.996

[a] Experimental proton affinities ΔH^{298} are given in parentheses and are based on data taken from Lias *et al.* (1988).

[b] MP2/6-31 +G(d, p) proton affinities are not usually quantitatively accurate, but for the 4-R-pyridines they are within 1 kcal mol^{-1} of the experimental values, except for X = NH_2.

[c] ΔE_e is the electronic binding energy of the complex.

proton-shared hydrogen bonds exhibit multiple strong bands in the IR spectrum between 600 and 1700 cm^{-1}. The strongest band is dramatically shifted by 40–60% relative to the HCl monomer, and all bands have significantly increased intensities. The normal coordinate analysis shows that these bands are not simple perturbed Cl–H stretches but involve coordinated motion of the hydrogen-bonded chlorine, hydrogen and nitrogen atoms. How do these bands arise?

In complexes with proton-shared hydrogen bonds, the H–Cl bond is significantly lengthened and weakened. As a result, the H–Cl stretching force constant is reduced, and this leads to a dramatic reduction in the H–Cl stretching frequency. If the H–Cl stretching band is shifted into a region where the pyridine molecule absorbs, then coupling of the HCl stretch and pyridine vibrational modes can occur provided that these modes have the same symmetry (a_1 in C_{2v}). The relatively weak intramolecular modes in pyridine may then borrow intensity from the H–Cl stretching mode, with the result that several strong bands appear in the spectrum, with frequencies and intensities dependent on the extent of local oscillator coupling. This is an important observation since it demonstrates that it is not necessary to invoke the existence of double minima along the proton transfer coordinate in order to explain multiple strong bands in the experimental vibrational spectra of some hydrogen-bonded complexes. There are no double minima along this coordinate in any of the complexes of HCl with the 4-R-pyridines.

Substitution of S^- and O^- in the 4 position of pyridine so increases the base

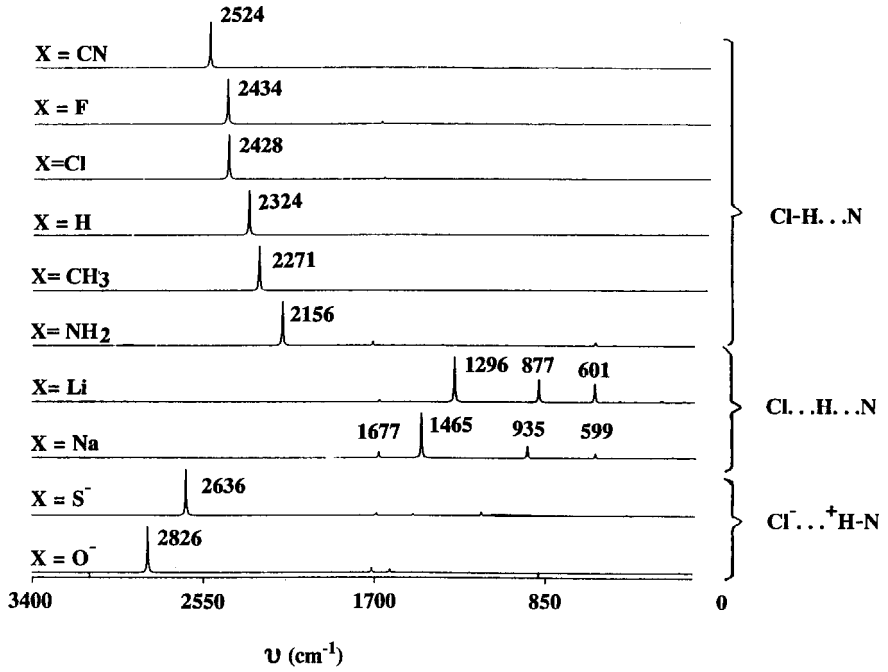

Figure 1. The computed spectra of ClH : 4-R-pyridine complexes. Except for the pyridine modes which couple to the motion of the hydrogen-bonded proton, the bands of the substituted pyridine are not visible on this scale. (From Del Bene *et al.* (1996).)

strength that proton transfer occurs. The computed vibrational spectra of the resulting hydrogen-bonded ion pairs again have single strong bands. However, the motion of the proton in these complexes is better described as a perturbed N–H stretching motion in an $N{-}H^{+}\cdots Cl^{-}$ hydrogen bond. The strong bands in the complexes ClH : 4-S^{-}-pyridine and ClH : 4-O^{-}-pyridine are found at 2636 and 2826 cm^{-1}, and are shifted to lower frequency by about 1050 and 900 cm^{-1} respectively relative to the corresponding pyridinium ions. The magnitude of these shifts is comparable with shifts of the HCl band in complexes with traditional $Cl{-}H\cdots N$ hydrogen bonds.

The relationship between the computed structure of a hydrogen-bonded complex and its computed harmonic spectrum is evident from the HX : 4-R-pyridine complexes. Complexes with traditional hydrogen bonds have computed harmonic spectra typical of this structure type, while complexes with proton-shared hydrogen bonds have dramatically different spectra, exhibiting multiple low-frequency strong bands. The computed results also demonstrate important relationships among properties such as the proton affinity of the substituted pyridine, the binding energy of the complex, the intermolecular distance, the X–H distance in the complex and the frequency shift of the X–H band. However, while the computed results for the HX : 4-R-pyridine complexes are internally consistent, there is a problem. Comparison of the computed harmonic spectra of these complexes with experimental spectra indicates that proton-shared hydrogen bonds appear earlier in the series experimentally (i.e. at lower proton affinity of the base) than predicted from the calculations. For example, HCl : pyridine has an experimental spectrum typical of complexes with proton-shared hydrogen bonds, (W. B. Person and K. Szczepaniak 1997, private communication) but the computed spectrum of this complex is that of a complex with a traditional hydrogen

bond. It should be noted that there is also an apparent discrepancy between experimental structural and spectroscopic data for this same complex, since the reported gas-phase structure of HCl:pyridine is also suggestive of a traditional hydrogen bond (Cooke *et al.* 1998). Similar discrepancies between experimental gas-phase structure and experimental argon matrix spectra, and between experimental and computed harmonic IR spectra, are found for the $BrH:NH_3$ complex (Del Bene *et al.* 1997a, Barnes and Legon 1998). In both cases, the computed MP2/6-31 +G(d,p) structures are in agreement with the experimental gas-phase structures, but the computed harmonic IR spectra are drastically different from experiment. It does not appear that the discrepancies between computed harmonic and experimental IR spectra are due primarily to inadequacy of the MP2/6-31 +G(d,p) level of theory, since calculations done at higher levels of theory with larger basis sets yield essentially the same results. What are the origins of these discrepancies? There are two possible causes: anharmonicity and a matrix effect.

5. Calculation of anharmonic frequencies

5.1. *An overview of the calculation of vibrational energy levels*

This section deals with the calculation of purely vibrational energy levels, that is levels for which the total angular momentum of the system is zero ($J = 0$). There have been a number of reviews of such methods (Handy 1989, Tennyson 1992, Csaszar and Mills 1997) and only a brief theoretical overview will be provided here.

5.1.1. *Coordinates*

Regardless of the method used to calculate the vibrational eigenvalues, some representation of the molecular potential energy surface is required. It is always desirable to write the potential energy surface for a nonlinear N atom system in terms of $3N-6$ internal coordinates, with the choice of coordinates being appropriate for the particular system. For a triatomic ABC molecule, the choices include the following:

(*a*) the internal valence coordinates r_1, r_2 and the included angle θ (Carter and Handy 1982);
(*b*) Jacobi, or scattering, coordinates R, r, θ (Tennyson and Sutcliffe, 1985, Bowman *et al.* 1989);
(*c*) hyperspherical coordinates for the stretching motions r_i and ϕ, together with the bond angle θ (Frey and Howard 1985, Zuniga *et al.* 1996);
(*d*) symmetry coordinates r_1+r_2, r_1-r_2, r_3 (Ishtwan and Collins 1991, Collins and Parsons 1993);
(*e*) Radau coordinates (Johnson and Reinhardt 1986, Bačić *et al.* 1988).

Curvilinear internal coordinates are preferable because they give a more accurate representation of the potential energy surface (Hoy *et al.* 1972) and ensure that the potential surface is invariant to rotation and translation (Ishtwan and Collins 1991). For this latter reason, it is also desirable to write the kinetic energy operator in terms of internal coordinates. Using the chain rule (with the aid of computer algebra programs for larger systems) it is possible to derive the kinetic energy operator for any well defined coordinate system (Handy 1987). For example, for a triatomic ABC

molecule using the AB and BC bond lengths as r_1 and r_2 and the ABC included angle as θ, the kinetic energy operator may be written in atomic units as (Carter and Handy 1982).

$$\begin{aligned} T = & -\frac{1}{2\mu_1}\frac{\partial^2}{\partial r_1^2} - \frac{1}{2\mu_2}\frac{\partial^2}{\partial r_2^2} - \frac{1}{2}\left(\frac{1}{\mu_1 r_1^2} + \frac{1}{\mu_2 r_2^2} - \frac{2\cos\theta}{m_B r_1 r_2}\right) \\ & \times \left(\frac{\partial^2}{\partial\theta^2} + \cot\theta\frac{\partial}{\partial\theta}\right) - \frac{1}{m_B}\frac{\sin\theta}{r_1 r_2}\frac{\partial}{\partial\theta} + \frac{\cos\theta}{m_B} \\ & \times \left(\frac{1}{r_1}\frac{\partial}{\partial r_2} + \frac{1}{r_2}\frac{\partial}{\partial r_1}\right) - \frac{\cos\theta}{m_B}\frac{\partial^2}{\partial r_1 \partial r_2} + \frac{\sin\theta}{m_B}\frac{\partial}{\partial\theta} \\ & \times \left(\frac{1}{r_1}\frac{\partial}{\partial r_2} + \frac{1}{r_2}\frac{\partial}{\partial r_1}\right) - \frac{\cos\theta}{m_B r_1 r_2} + V, \end{aligned}$$

where

$$\frac{1}{\mu_1} = \frac{1}{m_A} + \frac{1}{m_B}, \quad \frac{1}{\mu_2} = \frac{1}{m_B} + \frac{1}{m_C},$$

and m_X is the mass of atom X. Expressing the Hamiltonian in terms of internal coordinates also facilitates the choice of appropriate basis functions, since the wavefunction is better represented as a direct product of functions of the internal coordinates than Cartesian coordinates. To minimize the computational effort involved in obtaining the vibrational eigenvalues it is important to choose basis functions which best approximate the exact wavefunction. The disadvantage of internal coordinates is the complexity of the kinetic energy operator, as evidenced in the above equation. This disadvantage may be minimized by choosing basis functions for which the kinetic energy matrix elements may be computed analytically or with minimum numerical effort. A further disadvantage is that the transformation from a total of $3N$ coordinates to three translational, three rotational and $3N-6$ internal coordinates inevitably introduces singularities into the Hamiltonian. Thus, not all choices of internal coordinates are actually usable, and it may be that no one coordinate choice is appropriate for the range of atomic configurations sampled in a given problem (Sutcliffe and Tennyson 1991, Thompson *et al.* 1998). General solutions to this problem have been proposed (Thompson *et al.* 1998), but these have yet to be tested in the context of realistic vibrational calculations.

5.1.2. *The potential energy surface*

The most computationally viable method for obtaining a molecular potential energy surface is to expand the surface as a power series about some equilibrium configuration. A Dunham (1932)-type representation is often used:

$$V = \sum c_{abc} (\Delta r_1)^a (\Delta r_2)^b (\Delta\theta)^c$$

where Δr_1, Δr_2 and $\Delta\theta$ are the bond length and bond angle changes with respect to equilibrium. The potential energy is commonly represented by a Taylor series expansion in normal coordinates (Papousek and Aliev 1984) or Morse coordinates (Meyer *et al.* 1986). The expansion coefficients are identified as force constants, and

the force field in which the atoms move can be obtained from *ab initio* calculations or from experiment. The *ab initio* prediction of anharmonic force fields has been an active research area for almost 20 years, fuelled by the development of analytic methods for the evaluation of the derivatives of the potential energy surface (Botschwina 1979, Bock *et al*. 1980, Botschwina and Sebals 1983, Pulay *et al*. 1983, Kondo *et al*. 1984, Gaw and Handy 1985, 1986, Dunn *et al*. 1986, Bartlett *et al*. 1988, Gaw *et al*. 1988). At present it is possible to calculate *ab initio* representations of the potential energy surface through to fourth order using analytic techniques (Gaw and Handy 1985). Sixth-order force fields have been calculated numerically for small molecules (Csaszar 1992, 1994). There is also an extensive literature relating to the experimental calculation of anharmonic force constants (Mills 1972, 1974).

In principle it is possible to describe a global molecular potential energy surface using a Taylor expansion about equilibrium. In practice, however, a satisfactory method for extrapolating the potential to arbitrary molecular configurations has yet to be found (Tennyson 1992). The alternatives are to investigate the chemically relevant regions of the potential energy surface using an appropriate *ab initio* method and then to fit a suitable functional form (Truhlar 1981, Murrell *et al*. 1984) or to interpolate among known data points (Jordan *et al*. 1995, Del Bene *et al*. 1997a).

5.1.3. *Perturbation theory*

The simplest description of the low-lying vibrational states in bound molecules is the harmonic approximation in which only a second-order Taylor expansion of the potential is considered. Molecules are assumed to undergo small-amplitude motion about some equilibrium geometry, and the vibrational wavefunctions are taken as products of one-dimensional harmonic oscillators (Wilson *et al*. 1980). This simple method is often extremely useful and can provide a qualitatively correct picture for many molecules (Hehre *et al*. 1986, Bartlett and Stanton 1994). The simple harmonic model can be improved using perturbation theory. In this approach, higher-order terms in the Taylor expansion of the molecular potential energy surface are used to correct the harmonic energy levels. The most commonly used perturbational method is second-order vibrational perturbation theory (Papousek and Aliev 1984). In this method, only quartic terms in the anharmonic force fields are required, and the anharmonic corrections to the vibrational energy levels are relatively simple. It is also possible to take into account the effects of cubic (Fermi) and quartic (Darling–Dennison) resonances within the framework of the calculations. (For a general discussion of the method see Csaszar and Mills (1997).) There are a number of public domain computer programs that perform second-order vibrational perturbation theory calculations. One of the most commonly used packages is SPECTRO (Gaw *et al*. 1991), which has been used to study a wide range of small molecules (for example Lee (1997)). A compilation of species for which full anharmonic (at least quartic) force fields have been determined have also been provided (Csaszar and Mills 1997).

The main advantage of the perturbative approach is that the information required about the potential energy surface is limited. It is computationally much easier to calculate even quartic force constants about equilibrium than to elucidate an entire potential energy surface. The second-order vibrational perturbation theory method is also much simpler and more tractable than a full variational method. However, because perturbative methods rely on accurate expansions of the potential about equilibrium, they are only appropriate for systems with well defined minima. A

perturbative approach is not appropriate when multiple minima exist on the potential surface, or when the minimum is not well defined as, for example, in weakly bound complexes (Handy 1989). Further, perturbative methods are not appropriate for cases in which the amplitude of vibrational motion is large (Tennyson 1992). In particular, the method is not appropriate for complexes with 'floppy' hydrogen bonds (LeRoy and Carley 1980).

5.1.4. *Variational methods*

The variational method is the only method free from all the fundamental obstacles to the accurate and general treatment of the vibrational problem. In this method the potential energy surface is globally defined by some functional form V and some basis set expansion is used. Typically, the wavefunction Ψ is expanded as a direct product of one-dimensional oscillator functions ϕ in the internal coordinates q_i:

$$\Psi = \sum c_{\mathrm{I}} \Phi_{\mathrm{I}},$$

where

$$\Phi_{\mathrm{I}} = \prod_{\mathrm{i}}^{3N-6} \phi_{Ii}(q_i).$$

For example, in a triatomic system $\phi(r_1)$ and $\phi(r_2)$ may be Morse oscillator functions and $\phi(\theta)$ may be a Legendre function. The Hamiltonian matrix is then defined in terms of the basis representation Φ_I as

$$H_{IJ} = \langle \Phi_I | H | \Phi_J \rangle$$

and the vibrational energy levels are calculated as the eigenvalues of the secular matrix:

$$\langle \Phi_I | H - W | \Phi_J \rangle = 0.$$

The resulting eigenvectors provide a representation of the vibrational wavefunctions within the given basis set. Since the ith eigenvalue is an upper bound on the ith exact eigenvalue (MacDonald 1933), it is possible to converge the vibrational states as the number of basis functions is increased. This method has been labelled the finite basis representation (FBR) (Bačić and Light 1989). For a given basis set, the secular (Hamiltonian) matrix elements are obtained by integrating over all coordinates. While some of the required integrals may be analytic (depending on the choice of basis functions and the form of the potential energy surface) many must be evaluated numerically, typically using Gaussian quadrature.

5.1.5. *Discrete variable representations*

The discrete variable representation (DVR) is a finite-element method that has been applied to the nuclear Schrödinger equation. The method has been extensively developed in the context of rovibrational problems by Light and coworkers, and a comprehensive review has been provided by Bačić and Light (1989). A critique of both the FBR and the DVR methods has also been provided by Tennyson (1992, and references therein). A DVR is obtained from a corresponding FBR. Indeed, when properly defined, DVRs and FBRs may be considered as equivalent pointwise and

spectral representations with orthogonal transformations between them, that is the DVR and FBR matrices are isomorphic. For example, for a coordinate x associated with an FBR $\phi_n(x)$, $n = 1, N$, the one-dimensional DVR $|x_\alpha\rangle$, $\alpha = 1, N$, is given by

$$|x_a\rangle = \sum_{n=1}^{N} T_{nx}\ \phi_n(x),$$

where $\mathbf{T}$ is the transformation matrix that diagonalizes the coordinate matrix $\mathbf{X}$, expressed in the DVR representation:

$$\boldsymbol{X}^{\mathrm{DVR}} = \boldsymbol{T}_x^t\ \boldsymbol{X}\boldsymbol{T}_x$$

with $\mathbf{X}^{\mathrm{DVR}}$ diagonal. The eigenvalues x_α, $\alpha = 1, N$, of $\mathbf{X}$, are the DVR grid points. If the basis functions $\phi_n(x)$ are orthogonal polynomials, then the DVR points are the Gaussian quadrature points for the polynomial basis functions (Bačić and Light 1989). The fundamental assumption inherent in the DVR method is that the potential matrix is diagonal. This approximation is based on the accuracy of Gaussian quadrature. Thus, the DVR Hamiltonian may be easily constructed provided that the basis set representation of the kinetic energy is simple. Basis functions are usually chosen so that the kinetic energy matrix is no worse than tridiagonal (Wei and Carrington 1992). Although the DVR method is not strictly variational, it has very strong links with the basis set method discussed above and is subject to the same pitfalls. Thus, the DVR method shall be considered a variational method.

The computational bottleneck in variational calculations is the diagonalization of the secular matrix. Therefore, the number of basis functions used (the dimension of the secular matrix) is critically important. Indeed, the major disadvantage of variational methods lies in the fact that, as either the number of atoms or the maximum energy of the eigenvalues increases, the number of basis functions becomes extremely large. (For example, when the number of atoms changes from three to four, the wavefunction becomes a direct product of six instead of three one-dimensional functions.) Further, as the molecule becomes larger, it becomes more difficult to choose appropriate expansion functions for low-frequency vibrations such as angle bends and torsional motions (Handy 1989).

There are, however, a number of promising avenues that have allowed variational methods to be applied to larger systems and/or higher energies. These include the following:

(*a*) the use of iterative diagonalization methods that allow very large basis sets to be used without requiring the explicit storage of the Hamiltonian matrix; these techniques are variations of the Lanczos (1950) method (Cullum and Willoughby 1985), which converges sparse regions of the spectrum toward more dense regions and is particularly useful in determining low-energy vibrational eigenvalues (Bramley and Carrington 1993, Antikainen *et al.* 1995);

(*b*) the use in denser regions of the spectrum of various filtering techniques which are either time dependent (Feit *et al.* 1982, Neuhauser 1990, 1994, Wall and Neuhauser 1995) or time independent (Iung and Leforestier 1992, 1995, Kono 1993, Huang *et al.* 1994, 1996, Kouri *et al.* 1995, Mandelshtam and Taylor 1995, Mandelshtam *et al.* 1995, 1996, Wyatt 1995; Chen and Guo 1996, Parker *et al.* 1996, Smith 1996, Yu and Smith 1997);

(*c*) basis set optimization, that is the optimization of a reduced set of equations prior to coupling to additional degrees of freedom. This method was first used successfully by Carter and Handy (1986) in a FBR application and has been used subsequently for calculating 'potential-optimized' DVRs (Echave and Clary 1992, Bramley and Carrington 1993). The major strength of the DVR method is that it is easily amenable to such contraction techniques and leads to the construction of very compact bases.

The variational method has been applied to investigate a range of tri-atomic and tetra-atomic species. Recent examples are those reported by Carter *et al.* (1995), Antikainen *et al.* (1995), Schwenke (1996), Koput and Carter (1997), Rosenstock *et al.* (1998) and Schmidt *et al.* (1998).

5.1.6. *Vibrational self-consistent field theory*

An alternative to the full use of the variational method has been suggested by Bowman (1978, 1986) and by Dunn *et al.* (1986) and Pulay (1990). This method is analogous to the self-consistent field (SCF) method used in electronic structure theory and has a similar direct configuration interaction (CI) formalism. The method obtains vibrational eigenstates iteratively and is not as computationally intensive as a full matrix diagonalization. The method, however, is based on an expansion in dimensionless normal coordinates and is suited to the case in which a perturbative expansion of the potential energy surface about equilibrium is an appropriate representation of the surface. In the case of a loosely bound hydrogen-bonded complex, however, the appropriate choice of normal coordinates may be ambiguous, and the very anharmonic nature of the potential may make convergence slow. Dimensionless normal mode coordinates are also not well suited to cases where it is difficult to assign good quantum numbers to each eigenstate (Chang *et al.* 1986). Further, it has been shown that the method is not suitable for describing the bending vibrational motions in water (Csaszar and Mills 1997).

5.1.7. *Scattering methods*

Calculating bound-state vibrational eigenvalues can be viewed as a special case of scattering calculations. Instead of one unbound degree of freedom all degrees of freedom are bound, and formalisms used in scattering calculations may be applied to vibrational problems. In the general scattering problem the bound modes are treated variationally as in section 5.1.4, and the eigenvalues for the bound motions are calculated as the value of the scattering (unbound) coordinate changes from zero to infinity. The scattering component of the overall wavefunction is a translational function that exponentially decays at short distances where it is within a potential wall and is asymptotically described by a plane wave as the interaction potential tends to zero and the moieties separate. The total wavefunction for the system is calculated by propagating from the classically forbidden region and matching boundary conditions with the asymptotic solution.

If the system being studied is a bound molecule, the scattering coordinate describes bound vibrational motion and the 'scattered' component of the wavefunction exponentially decays at large distance, where it is again within a potential wall. The vibrational eigenvalues of a molecule can be calculated using a scattering formalism by, for example, simultaneously propagating the wavefunction at a given scattering energy from both classically forbidden regions (at short and large distances). The propagated wavefunctions are examined for continuity in a classically allowed region

of the potential and the scattering energy is adjusted until the wavefunction has the required continuity at this matching coordinate. This value of the scattering energy then corresponds to a vibrational eigenvalue for the system. Bound-state wavefunctions may be calculated using either the time-dependent (Zhang and Zhang 1995, Wu *et al.* 1995; Hartke and Werner 1997, Mahapatra *et al.* 1998, Qui *et al.* 1998) or the time-independent (Clary *et al.* 1997) Schrödinger equations. As noted above, either a FBR or a DVR may be used to describe the bound degrees of freedom in any of these calculations.

5.1.8. *Quantum diffusion Monte Carlo method*

A final non-variational method that is appropriate to weakly bound complexes is the quantum diffusion Monte Carlo (QDMC) method. This is a fully quantum mechanical approach that, although initially developed in the context of electronic structure calculations, may be applied to the vibrational problem. In the QDMC method the Schrödinger equation is written in imaginary time τ and resembles a diffusion equation with a growth (or decay) term. In this formalism the wavefunction may be considered as a sum of transients and, if appropriate conditions are chosen, the wavefunction will decay to zero at large τ, with the longest-lasting transient corresponding to the ground state (Suhm and Watts 1991). This approach was first applied to molecular vibrations in 1985 by Miller *et al.* (1985) and then by Coker and Watts (1987), and a comprehensive review of the method has been provided by Suhm and Watts (1991).

There are a number of disadvantages associated with QDMC. First, the statistical errors in a QDMC calculation may be large. It is possible, however, to improve the efficiency of the QDMC algorithm significantly by using importance sampling (Reynolds *et al.* 1982, Suhm and Watts 1991). Another disadvantage is that, unlike variational calculations, QDMC treats only a single state at a time, and this state corresponds to the lowest-energy state compatible with the chosen boundary conditions. Thus, excited-state QDMC calculations are non-trivial. Two methods have been introduced to obtain excited-state energies. The first involves a fixed-node algorithm, where a nodal surface is physically introduced into the calculation. (Anderson 1975, 1976, 1980). The second involves orthogonalization, in which the state of interest is constrained to be orthogonal to all previously determined states with the same symmetry (Coker and Watts 1986, Quack and Suhm 1990, Sun and Watts 1990). It is also possible to gain information about excited states by probing the transients in the wavefunction (Ceperley and Alder 1981, Ceperley and Bernu 1988, Bernu *et al.* 1990, Blume *et al.* 1997a,b).

The fixed node constraint is very effective in determining the lowest-energy excited state of each symmetry. This makes it quite useful for systems with high symmetry, but not as useful for systems with little or no symmetry. The orthogonalization constraint, although conceptually simple, is computationally difficult and can suffer from a lack of resolution. However, Gregory and Clary (1995) have developed a rigid-body QDMC technique that can directly calculate tunnelling splittings in a single calculation. Another approach suggested recently is the projection operator imaginary time spectral evolution (POITSE) method (Blume *et al.* 1997a,b). This method involves the calculation of imaginary time correlation functions that are then subject to inverse Laplace transforms. Excited states are isolated using specific projection operators. To date the method has only been applied to model systems (Blume *et al.* 1997a,b).

The major advantage of the QDMC method is that it does not involve matrix diagonalization and can therefore be applied to large systems. QDMC also does not require explicit formulation of the wavefunction in terms of a basis representation. This makes the method appropriate for systems with very floppy modes that may be difficult to characterize. Indeed, QDMC has been widely used to calculate vibrational states and tunnelling splittings in van der Waals clusters, with many applications focusing on the intermolecular modes of water clusters (Gregory and Clary 1995, 1996, Gregory 1998, Sabo *et al.* 1998).

5.2. *Reduced dimensional calculations*

The evaluation of the anharmonic A−H stretching frequency (proton-stretching frequency) in a hydrogen-bonded complex is, in general, too complicated a problem to be dealt with in its complete dimensionality. The complications lie both in the nature of the vibrational calculation itself and in the *ab initio* elucidation of the potential energy surface. It is possible, however, to perform anharmonic calculations on a smaller number of active degrees of freedom. For example, the simplest possible anharmonic calculation would be performed in the single dimension corresponding to the proton-stretching mode. Two-dimensional calculations allowing for coupling between the proton stretch and the heavy-atom (dimer) stretch are also feasible, as are three- or four-dimensional calculations in which bending or inversion modes are coupled to the proton and dimer stretches. Since it has been shown that coupling between the proton and dimer stretching modes can be significant in some complexes, the method for treating the anharmonic two-dimensional vibrational problem will be discussed first. The first two-dimensional anharmonic treatment of vibration performed in this laboratory was carried out on $BrH:NH_3$ which, because of its small size, made a thorough systematic study feasible (Del Bene *et al.* 1997a).

The method used for the evaluation of two-dimensional anharmonic vibrational frequencies in hydrogen-bonded complexes is that outlined by Wei and Carrington (1992). For a collinear A–B–C system the two-dimensional model vibrational Hamiltonian is given by

$$H = -\frac{\hbar^2}{2\mu_1}\frac{\partial^2}{\partial R_1^2} - \frac{\hbar^2}{2\mu_2}\frac{\partial^2}{\partial R_2^2} + \frac{\hbar^2}{m_B}\frac{\partial^2}{\partial R_1\,\partial R_2} + V(R_1, R_2)$$

where R_1 is the AB bond length, R_2 is the BC bond length, $1/\mu_1 = 1/m_A + 1/m_B$, $1/\mu_2 = 1/m_B + 1/m_C$ and m_X is the mass of the moiety X. In $BrH:NH_3$, for example, A was identified as NH_3, B as the hydrogen atom, and C as the bromine atom, with R_1 representing the distance from hydrogen to the centre of mass of NH_3, and R_2 the Br–H distance. In $BrH:NH_3$, the hydrogen bond is exactly linear (C_{3v} symmetry), and no bending motion is allowed in the two-dimensional treatment.

The method of choice for solving the two-dimensional nuclear vibrational problem involves DVRs of the wavefunction. The wavefunction is expanded in internal coordinates and Hamiltonian matrix elements are calculated at appropriate quadrature points. The DVR points themselves can also be adapted to the potential surface, yielding a potential optimized DVR scheme. The strength of the DVR method is that the potential matrix is always diagonal. If appropriate basis functions are used, the kinetic energy matrix is also simple. This is the case for bond-stretching basis functions, where the tridiagonal Morse basis is extremely useful because it yields analytic tridiagonal Hamiltonian matrix elements.

The potential energy surface $V(R_1, R_2)$ needed in the two-dimensional treatment of vibration can be constructed from initial grids of *ab initio* data points using both interpolating and extrapolating functions, as described for $BrH:NH_3$ (Del Bene *et al.* 1997a). Converged anharmonic frequencies can be obtained provided that sufficient data points are available and that interpolations and extrapolations are done carefully. Since this method describes a reduced potential energy surface rather than relying on an expansion about a minimum on the surface, it is better suited to computing anharmonic frequencies for hydrogen-bonded complexes, particularly if there is significant coupling between two modes. Such coupling has been shown to be significant if a second region on the surface is accessible in either the ground or the first excited state of the proton-stretching mode.

In one dimension the calculation of the anharmonic frequency simplifies significantly. The one-dimensional Hamiltonian is

$$H = -\frac{\hbar^2}{2\mu}\frac{\partial^2}{\partial R^2} + V(R),$$

where the coordinate R parameterizes a particular slice along the potential surface and μ is the appropriate reduced mass. There are several one-dimensional slices that could be used for the anharmonic calculation, but the one that is well defined and an obvious choice is the curve generated from the normal coordinate displacement vector for the proton-stretching band obtained from the harmonic treatment. The potential can be defined by a one-dimensional spline interpolation through a discrete set of *ab initio* energies calculated along the normal coordinate displacement vector, and polynomial extrapolation of the potential outside the initial data set. As previously, tridiagonal Morse functions can be used to expand the vibrational wavefunctions.

Hydrogen-bonded complexes contain additional vibrational degrees of freedom that may influence their experimental spectra. Foremost among these is the hydrogen-bond-bending mode. The bending coordinate for a pseudo-three-atom system ABC with no overall rotational motion can be included in the Hamiltonian:

$$\begin{aligned} H(R_1, R_2, \theta) = {} & -\frac{\hbar^2}{2\mu_1}\frac{\partial^2}{\partial R_1^2} - \frac{\hbar^2}{2\mu_2}\frac{\partial^2}{\partial R_2^2} \\ & -\frac{\hbar^2}{2}\left(\frac{1}{\mu_1 R_1^2} + \frac{1}{\mu_2 R_2^2} - \frac{2\cos\theta}{m_B R_1 R_2}\right)\left(\frac{\partial^2}{\partial\theta^2} + \cot\theta\frac{\partial}{\partial\theta}\right) \\ & + \frac{\hbar^2\cos\theta}{m_B}\left(\frac{1}{R_1}\frac{\partial}{\partial R_2} + \frac{1}{R_2}\frac{\partial}{\partial R_1} - \frac{\partial^2}{\partial R_1 \partial R_2} - \frac{1}{R_1 R_2}\right) \\ & + \frac{\hbar^2\sin\theta}{m_B}\frac{\partial}{\partial\theta}\left(\frac{1}{R_1}\frac{\partial}{\partial R_2} + \frac{1}{R_2}\frac{\partial}{\partial R_1} - \frac{1}{R_1 R_2}\right) + V(R_1, R_2, \theta), \end{aligned}$$

where R_1 and R_2 are the A–B and B–C bond lengths respectively, θ is the ABC included angle, $1/\mu_1 = 1/m_A + 1/m_B$ and $1/\mu_2 = 1/m_B + 1/m_C$. As before, the bending motion can be described by a DVR scheme, in this case using a basis of Legendre polynomials evaluated at discrete grid points. This basis can be optimized to the potential by considering a purely bending one-dimensional Hamiltonian. The required kinetic energy matrix elements may be calculated using the properties of tridiagonal Morse and Legendre polynomials. Similar methods may, in principle, be used to describe

higher dimensionality or alternative curvilinear coordinates but, as the kinetic energy becomes more complex, numerical evaluation of matrix elements may be necessary. Work in this area is currently under way in our laboratory. It should be noted that the complexity of both the potential energy surface calculations and the calculation of vibrational eigenvalues increases dramatically with increasing number of dimensions. If n points are required for each dimension, then the number of single-point energy calculations needed is n^x, where x is the number of dimensions. Similarly, if k optimized basis functions are used per dimension considered, the overall direct product basis will contain k^x-functions. Because the calculation of vibrational eigenvalues requires the diagonalization of the Hamiltonian matrix, this calculation scales approximately as N^3, where N is the total number of basis functions used. Thus the scale of the problem increases enormously with increasing number of dimensions treated quantum-mechanically.

6. Results of one- and two-dimensional anharmonic treatments of vibration

6.1. *The BrH : pyridine spectrum*

The calculated MP2/6-31 +G(d, p) structure and the harmonic IR spectrum of BrH : pyridine is that of a complex with a proton-shared hydrogen bond, and the computed spectrum is in general agreement with the experimental argon matrix spectrum (Del Bene *et al.* 1997c; Sczcepaniak *et al.* 1997). Evident in both spectra are multiple intense bands below 1800 cm^{-1}. Analysis of the normal coordinate displacement vectors for these bands show that they arise from the Br–H stretching vibration coupled to local intramolecular modes of the pyridine ring. However, it is evident that there are differences between the computed harmonic spectrum and the experimental spectrum in both frequencies and intensities of strong bands, as evident in figure 2. The cause of this discrepancy can be seen from figure 3 to be the harmonic approximation. Figure 3 shows the parabola corresponding to the harmonic curve for proton motion for the strong band at 1561 cm^{-1} in the computed spectrum, and the potential curve for proton motion generated from the normal coordinate displacement vector for this same band. The normal coordinate curve is obviously not parabolic.

The potential curve generated from the normal coordinate displacement vector for the band at 1561 cm^{-1} was used to solve a one-dimensional nuclear vibrational equation for the Br–H stretch. The anharmonic v = 0 and v = 1 energy levels are shown in figure 3, together with the harmonic levels. The differences are evident, particularly in the energy of the v = 1 vibrational state. From these data, the ratio $\nu_{0\rightarrow 1}$(anharmonic)/$\nu_{0\rightarrow 1}$(harmonic) was computed to be approximately 0.72. This value was used to adjust the proton-stretching force constant k(anharmonic)/k(harmonic) = 0.72^2 = 0.52. The three internal coordinate force constants associated with the proton-stretching mode obtained from the harmonic calculation were then multiplied by 0.52, and the harmonic spectrum of BrH : pyridine was recomputed. The recomputed spectrum is shown in figure 4(*a*) and can be compared with the experimental matrix spectrum (figure 4(*c*)) and with the experimental integrated intensity sum spectrum obtained by combining the integrated intensities of weaker bands in the vicinity of a strong band into a single band (figure 4(*b*)). The agreement among the three spectra is remarkable and emphasizes the importance of anharmonicity of the Br–H stretching vibration in BrH : pyridine.

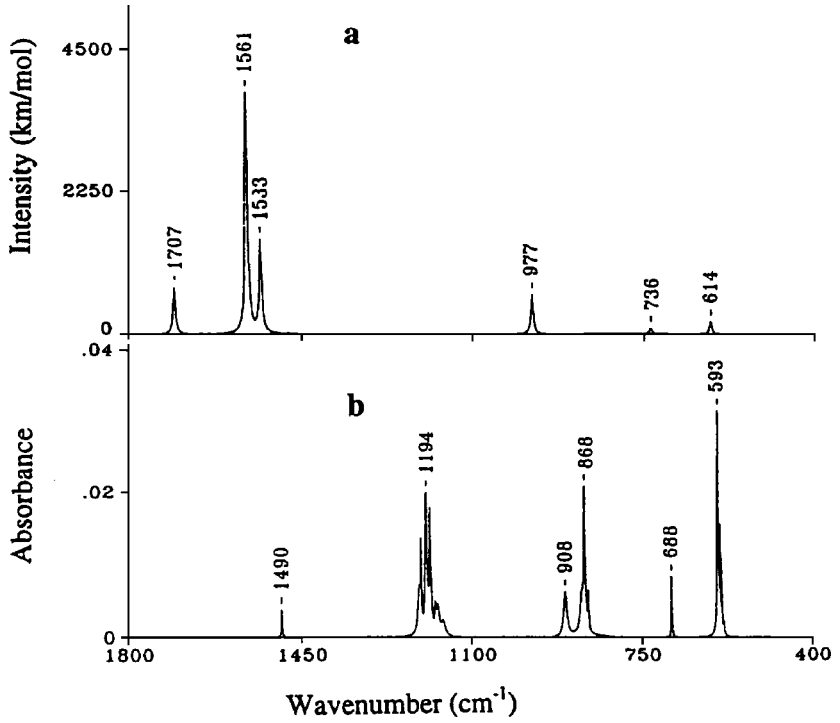

Figure 2. (*a*) Computed MP2/6-31 +G(d, p) harmonic spectrum and (*b*) the experimental argon matrix spectrum of BrH : pyridine extracted from the original experimental spectrum of the matrix containing the pyridine and HBr monomers and the complex. Reprinted with permission from Del Bene *et al.* (1997c). Copyright 1997 American Chemical Society.

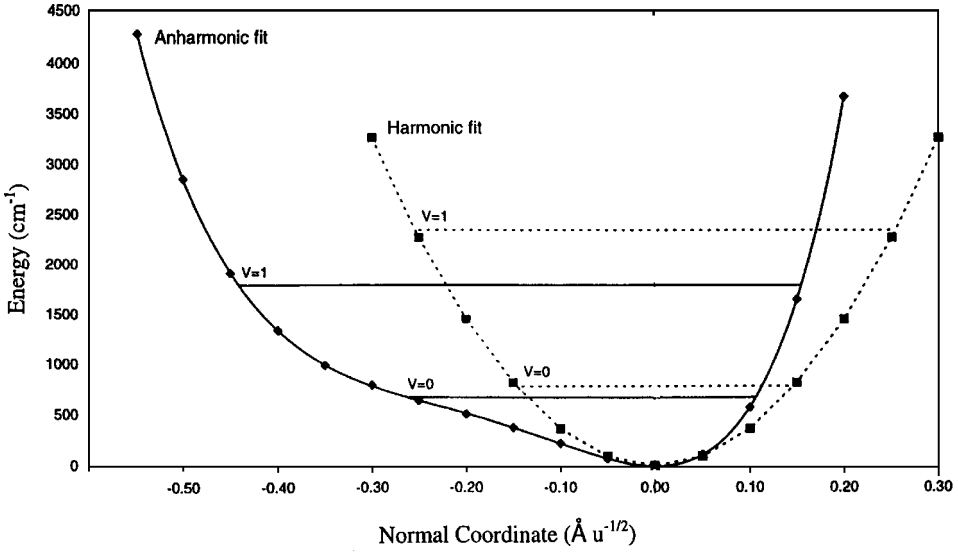

Figure 3. Potential curve for proton motion for BrH : pyridine along the normal coordinate for the band at 1561 cm^{-1}, with the v = 0 and v = 1 vibrational levels (——). The harmonic curve and vibrational levels (– – –) are shown for comparison. Reprinted with permission from Del Bene *et al.* (1997c). Copyright 1997 American Chemical Society.

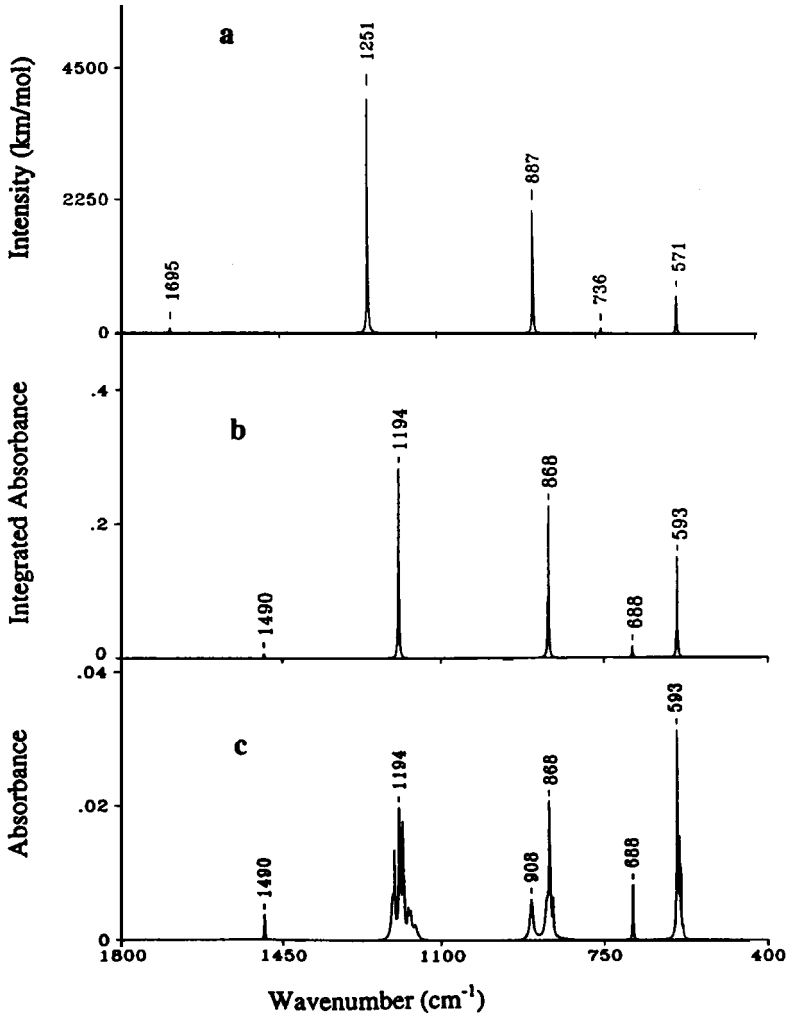

Figure 4. (*a*) Recomputed BrH : pyridine spectrum using the anharmonic proton stretching force constant, (*b*) the experimental integrated intensity spectrum of BrH : pyridine and (*c*) the experimental spectrum of this complex. Reprinted with permission from Del Bene *et al.* (1997c). Copyright 1997 American Chemical Society.

6.2. *The complexes XH : NH_3*

The computed MP2/6-31 +G(d, p) harmonic spectra of FH : NH_3 and BrH : NH_3 are compared with the corresponding experimental spectra obtained in argon matrices in figure 5. While the computed and the experimental spectra of FH : NH_3 are similar, there are significant discrepancies between the computed and the experimental spectra of BrH : NH_3. The investigation of the structures and IR spectra of the series of complexes XH : NH_3 for X = F, Cl and Br was pivotal to progress in understanding anharmonicity and matrix effects in hydrogen-bonded complexes (Del Bene *et al.* 1997a, Del Bene and Jordan 1998). The structures and spectra of these complexes will be discussed in turn.

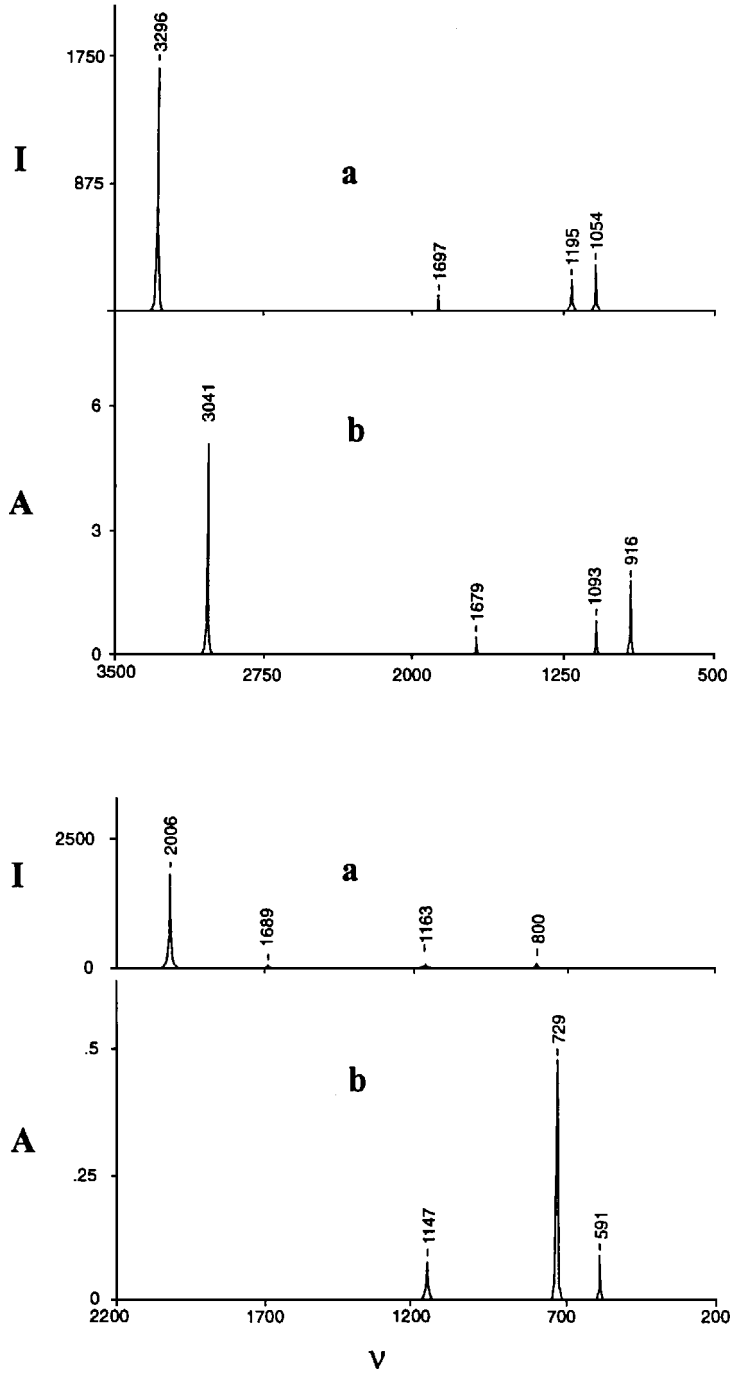

Figure 5. (*a*) The computed and (*b*) the experimental argon matrix spectra of FH : NH_3 (top) and BrH : NH_3 (bottom).

Table 5. Harmonic and anharmonic frequencies for the dimer- and proton-stretching modes in $XH:NH_3$ complexes at MP2/6-31 +G(d, p).

	Frequency (cm^{-1})		
	$FH:NH_3$	$ClH:NH_3$	$BrH:NH_3$
Proton stretch			
Harmonic	3296	2541	2006
Anharmonic			
One dimensional	2949	2278	1533
Two dimensional	2832	1869	888
Experimental	3041[a]	1371[b]	729[c]
Dimer stretch			
Harmonic	272	182	135
Anharmonic two dimensional	287	184	218

[a] From Johnson and Andrews (1982).
[b] From Barnes *et al.* (1984).
[c] From W. B. Person and K. Szczepaniak (1997, private communication).

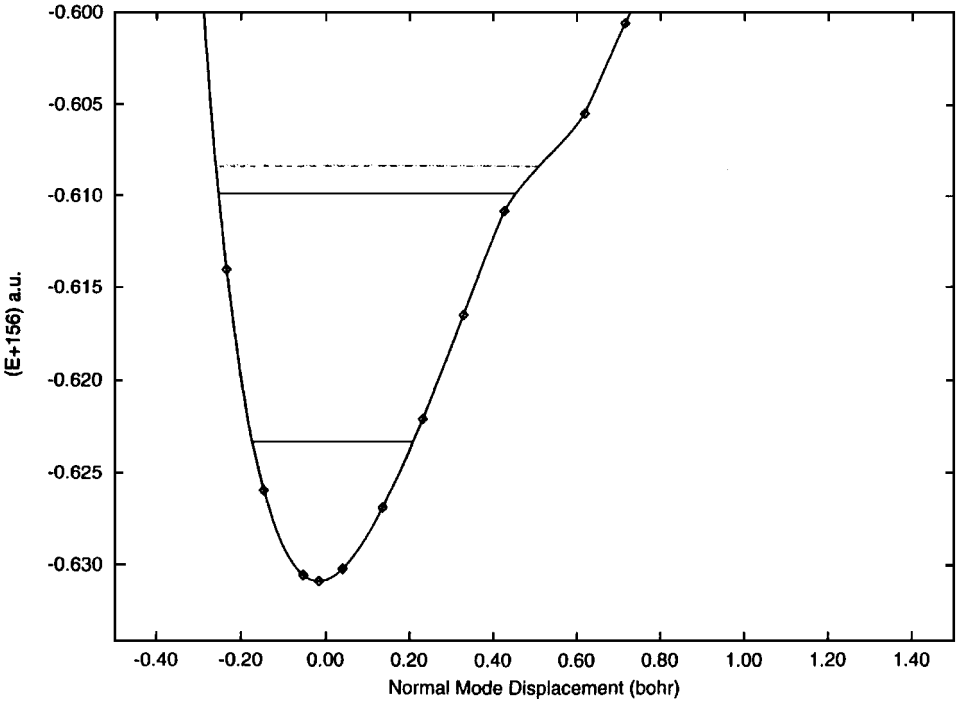

Figure 6. The potential curve for motion along the normal coordinate displacement vector for the harmonic proton stretching mode in $FH:NH_3$, where the v= 0 harmonic and anharmonic energies are identical: (——), anharmonic vibrational energy levels; (– – –), harmonic levels. (From Del Bene and Jordan (1998), with permission.)

6.2.1. *FH : NH*$_3$

The complex $FH:NH_3$ has C_{3v} symmetry, with a computed MP2/6-31 +G(d, p) intermolecular distance of 2.637 Å and an F–H distance of 0.963 Å. This complex has a computed structure and IR spectrum consistent with the presence of a traditional

F–H···N hydrogen bond. The computed spectrum exhibits a single strong F–H stretching band at 3296 cm^{-1}, 255 cm^{-1} higher than the experimental frequency measured in an argon matrix. This difference reflects primarily the anharmonicity of the F–H stretch in the HF monomer. The anharmonicity correction in HF is 176 cm^{-1} experimentally (Mills 1974) and 181 cm^{-1} at MP2/6-31 +G(d,p). The apparently larger correction in $FH:NH_3$ suggests that the F–H stretch in the complex is slightly more anharmonic than in the isolated HF molecule.

The anharmonic stretching frequencies obtained by solving one- and two-dimensional vibrational equations on the MP2/6-31 +G(d,p) surface for $FH:NH_3$ are reported in table 5. The one-dimensional frequency computed from the potential curve generated from the normal coordinate displacement vector for the F–H stretch in $FH:NH_3$ is 2949 cm^{-1}, which underestimates the experimental value by 92 cm^{-1}. The F–H stretching frequency obtained from the two-dimensional treatment is 2832 cm^{-1}, which underestimates the experimental by 209 cm^{-1}. The difference between the one- and two-dimensional frequencies arises from the small coupling between proton-stretching and dimer-stretching modes in the two-dimensional treatment. Although the computed harmonic F–H stretching frequency is too large and the anharmonic frequencies are too small, they are in reasonable agreement with experiment. Further improvement would require that the calculations be carried out at more sophisticated levels of theory.

Figure 6 shows the one-dimensional potential curve along the normal coordinate displacement vector for $FH:NH_3$, and the location of the $v = 0$ and $v = 1$ vibrational energies. As evident from this figure, the harmonic and anharmonic zero-point vibrational energies are essentially identical, while the $v = 1$ anharmonic level is slightly lower than the harmonic. Both vibrational levels are contained within the potential well. Figures 7 and 8 respectively show the square of the ground state ($v = 0$) and of the first excited state ($v = 1$) vibrational wavefunctions for the proton stretching mode superimposed on the $FH:NH_3$ MP2/6-31 +G(d,p) surface. These wavefunctions are centred over the potential minimum on the surface, and in both the ground and the first excited state the displacement of the proton from its equilibrium position is not large. The one- and two-dimensional plots illustrate graphically why the harmonic approximation works reasonably well for this complex.

6.2.2. *$ClH:NH_3$*

The computed structure of $ClH:NH_3$ has a traditional Cl–H···N hydrogen bond and the computed harmonic spectrum is consistent with this structure, showing a very strong band at 2541 cm^{-1}. The computed structure has a Cl–N distance R_e of 3.130 Å and is in agreement with the gas-phase structure reported by Legon (1993), with R_0 = 3.137 Å. However, the experimental IR spectrum of this complex is dramatically different from the computed spectrum. There are four strong bands between 1050 and 1450 cm^{-1} in the experimental IR spectrum that have been assigned to the $ClH:NH_3$ complex, although the specific nature of these is still open to discussion. Barnes *et al.* (1984) assigned the band at 1371 cm^{-1} to the Cl–H stretch, and this assignment will be used for comparison here.

The proton- and dimer-stretching frequencies obtained from one- and two-dimensional treatments of vibration on the MP2/6-31 +G(d,p) surface for $ClH:NH_3$ are reported in table 5. The square of the wavefunctions for the ground ($v = 0$) and first excited ($v = 1$) states of the proton stretching vibration are shown superimposed on the potential surface in figures 9 and 10 respectively. Although the ground-state

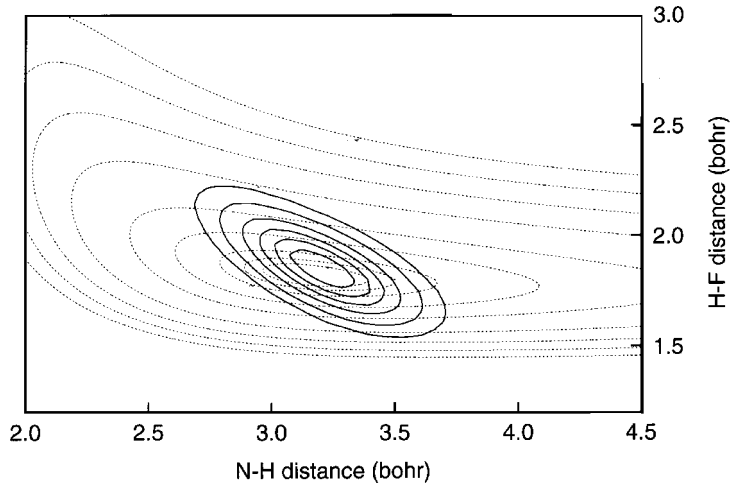

Figure 7. The square of the ground state vibrational wavefunction for $FH:NH_3$ shown superimposed on the MP2/6-31 +G(d, p) surface in the hydrogen-bonding region. The potential energy contours are at energies 0.0005, 0.001, 0.002, 0.003, 0.005, 0.01, 0.02, 0.03 and 0.04 au above the global minimum. (From Del Bene and Jordan (1998), with permission.)

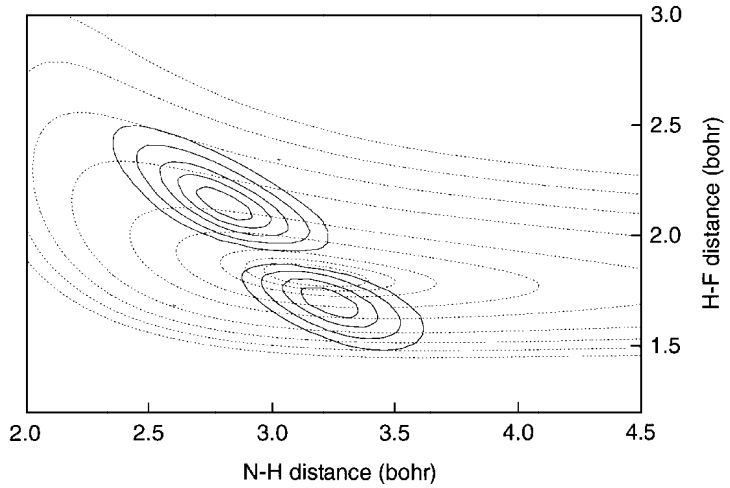

Figure 8. Square of the wavefunction for the first excited proton-stretching vibration of $FH:NH_3$ superimposed on the MP/6-31 +G(d, p) surface. (From Del Bene and Jordan (1998), with permission.)

wavefunction is centred over the well that describes the equilibrium complex, the excited-state wavefunction is displaced, suggesting that the proton undergoes large-amplitude motion in the v = 1 state as it samples the proton-shared region of the surface. (In the figures, the proton-shared region is located in the upper left of the plot, at shorter N–H and longer Cl–H distances.) The excited-state plot also suggests that there is coupling between proton and heavy-atom motions. This is supported by the computed expectation values of the Cl–H and Cl–N distances of 1.482 and 3.001 Å in the v = 1 state, compared with the ground-state expectation values of 1.346 and 3.134 Å respectively. The coupling between the proton and dimer-stretching modes in

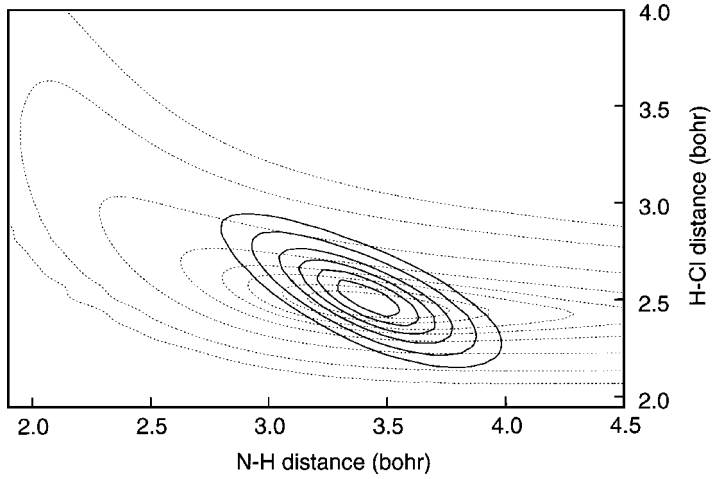

Figure 9. The square of the ground state vibrational wavefunction for $ClH:NH_3$ shown superimposed on the MP2/6-31 +G(d, p) surface in the hydrogen-bonding region. The potential energy contours are at energies 0.0005, 0.001, 0.002, 0.003, 0.005, 0.01, 0.02 and 0.03 au above the global minimum. (From Del Bene and Jordan (1998), with permission.)

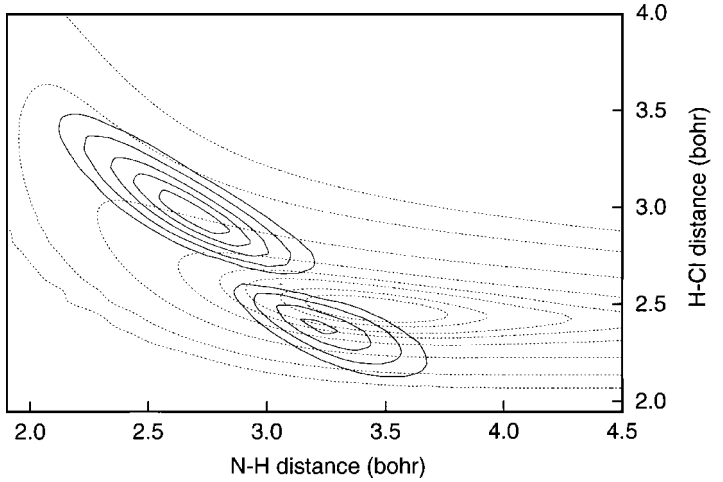

Figure 10. Square of the wavefunction for the first excited proton-stretching vibration of $ClH:NH_3$ superimposed on the MP/6-31 +G(d, p) surface. (From Del Bene and Jordan (1998), with permission.)

the excited state leads to a significant difference between the proton-stretching frequencies obtained from one- and two-dimensional anharmonic treatments of vibration. The anharmonic one-dimensional proton-stretching frequency computed from the potential curve generated from the normal coordinate displacement vector is 2278 cm^{-1}, compared with the two-dimensional value of 1869 cm^{-1}. However, while the two-dimensional proton-stretching frequency is significantly lower than the harmonic frequency of 2541 cm^{-1}, it is still about 500 cm^{-1} greater than the experimental frequency.

The agreement between the two-dimensional anharmonic frequency and the experimental frequency for the Cl–H stretch in $ClH:NH_3$ is expected to improve if a higher level of theory were used, and if the effect of the matrix could be evaluated.

(The matrix effect will be discussed in section 6.3.) It is noteworthy that the computed MP2/6-31 +G(d,p) harmonic and anharmonic stretching frequencies for the HCl monomer are too high relative to experiment and that, for the hydrogen halides HF, HCl and HBr, the difference between experimental and computed harmonic and anharmonic frequencies is greatest for HCl (Del Bene and Jordan 1998). This observation prompted a reinvestigation of HCl and the $ClH:NH_3$ complex using the larger aug´-cc-pVDZ basis set. (This basis is the aug-cc-pVDZ basis without diffuse functions on hydrogen atoms.) The computed harmonic and anharmonic MP2/aug´-cc-pVDZ frequencies for HCl are improved, and in better agreement with experiment. While the MP2/aug´-cc-pVDZ description of the equilibrium structure of $ClH:NH_3$ and the one- and two-dimensional plots for $ClH:NH_3$ obtained at MP2/aug´-cc-pVDZ are similar to the corresponding MP2/6-31 +G(d,p) plots, the MP2/aug´-cc-pVDZ one- and two-dimensional proton-stretching frequencies are reduced to 1842 and 1566 cm^{-1} respectively. The two-dimensional proton-stretching frequency is now only 200 cm^{-1} greater than the experimental argon matrix frequency.

6.2.3. *$BrH:NH_3$*

Two equilibrium structures of $BrH:NH_3$ exist on the MP2/6-31 +G(d,p) intermolecular surface. The more stable has a traditional Br–H···N hydrogen bond, with a computed Br–N distance R_e of 3.247 Å, in agreement with the experimental structure reported by Legon (1993) for which R_0 is 3.255 Å. The second minimum has a proton-shared Br···H···N hydrogen bond with a Br–N distance R_e of 2.971 Å. However, this structure is a Born–Oppenheimer minimum that converts to the more stable structure when the zero-point vibrational energy is added. The $BrH:NH_3$ surface is flat in the hydrogen-bonding region, and a valley connects the two minima. The complex with the traditional hydrogen bond has a computed harmonic IR spectrum with a strong band at 2006 cm^{-1}. The proton-shared complex has two strong very-low-frequency Br–H stretching bands at 414 and 387 cm^{-1}. Neither computed spectrum is in agreement with the experimental argon matrix spectrum, which exhibits a single strong Br–H stretching band at 729 cm^{-1} (Del Bene *et al.* 1997a).

Plots of the square of the vibrational wavefunctions for the ground (v = 0) and the first excited (v = 1) vibrational states of the proton-stretching mode obtained from the two-dimensional treatment of vibration on the $BrH:NH_3$ surface are shown superimposed on that surface in figures 11 and 12 respectively. The plot for the vibrational ground state is dramatically different from the corresponding plots for $FH:NH_3$ and $ClH:NH_3$. The square of the ground-state vibrational wavefunction is centred not over the potential well for the structure with the traditional hydrogen bond, but in the valley connecting this structure to the structure with a proton-shared hydrogen bond. Thus, both the traditional and the proton-shared regions of the surface are sampled even in the ground vibrational state. Figure 12 shows the extent to which the proton-shared region of the surface is further sampled in the v = 1 state.

As anticipated from figures 11 and 12, the anharmonic one- and two-dimensional proton-stretching frequencies for $BrH:NH_3$ are significantly different from each other, and from the harmonic frequency. The one-dimensional anharmonic Br–H stretching frequency obtained from the potential curve generated from the normal coordinate displacement vector at the global minimum is 1533 cm^{-1}, which is about 500 cm^{-1} lower than the harmonic frequency. The strong coupling between proton and dimer-stretching modes reduces this frequency in the two-dimensional treatment to 888 cm^{-1}, only 159 cm^{-1} higher than the experimental argon matrix value. The

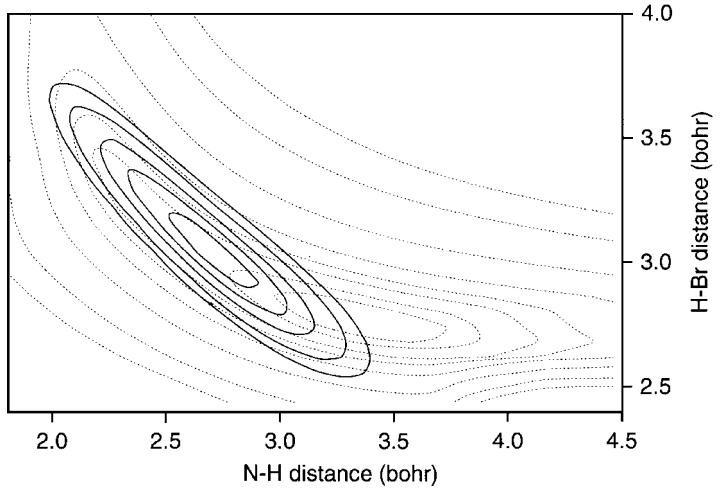

Figure 11. The square of the ground-state vibrational wavefunction for $BrH:NH_3$ shown superimposed on the MP2/6-31 +G(d, p) surface in the hydrogen-bonding region. The potential energy contours are at energies 0.0005, 0.001, 0.002, 0.003, 0.005, 0.01, 0.02 and 0.03 au above the global minimum. (From Del Bene *et al.* (1997a), with permission.)

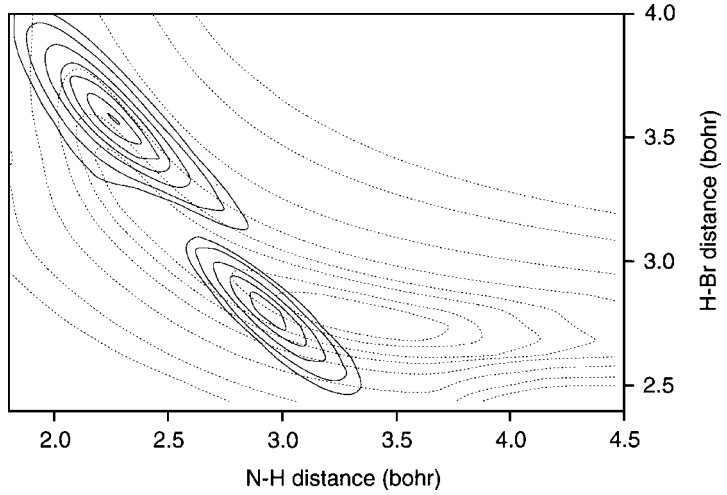

Figure 12. Square of the wave function for the first excited proton-stretching vibration of $Br:NH_3$ superimposed on the MP2/6-31 +G(d, p) surface. (From Del Bene *et al.* (1997a), with permission.)

remaining difference between the computed two-dimensional proton stretching frequency and the experimental argon matrix frequency may be due in part to the effect of the matrix.

6.3. *Matrix effects in* $XH:NH_3$ *complexes*

Initial attempts to evaluate matrix effects on the structures and spectra of hydrogen-bonded complexes were made by optimizing the structures of complexes in the presence of rare-gas atoms, and then computing their harmonic vibrational spectra (Del Bene *et al.* 1997a, b; Del Bene and Jordan 1998). The results for the $XH:NH_3$

Table 6. Selected MP2/6-31 +G(d,p) distances and harmonic vibrational frequencies and intensities for the proton-stretching mode in $XH:NH_3$ Complexes (HF, r = 0.926, v = 4122 and I = 126; HCl, r = 1.270, v = 3112 and I = 26; HBr, r = 1.407, ν = 2732 and I = 12).

Complex	X–N (Å)	X–H (Å)	X–P[a] (Å)	r[b] (Å)	ν (cm^{-1})	I (km mol^{-1})
$FH:NH_3$	2.637	0.963			3296	1696
$FH:NH_3$:3Ne	2.635	0.964	2.802	3.304	3289	1680
$FH:NH_3$:3Ar	2.629	0.964	1.322	3.416	3274	1580
$ClH:NH_3$	3.130	1.309			2541	1537
$ClH:NH_3$:3Ne	3.112	1.312	3.321	3.258	2498	1620
$ClH:NH_3$:3Ar	3.117	1.311	2.252	3.529	2502	1521
$BrH:NH_3$	3.247	1.462			2006	1948
$BrH:NH_3$:3Ne	2.966	1.746	3.055	3.197	703	4513
$BrH:NH_3$:3Ar	2.966	1.741	2.532	3.544	716	4617

[a] X–P is the distance from the halide to the plane of the inert-gas atoms.
[b] r is the perpendicular distance from the X–N axis to the inert-gas atom.

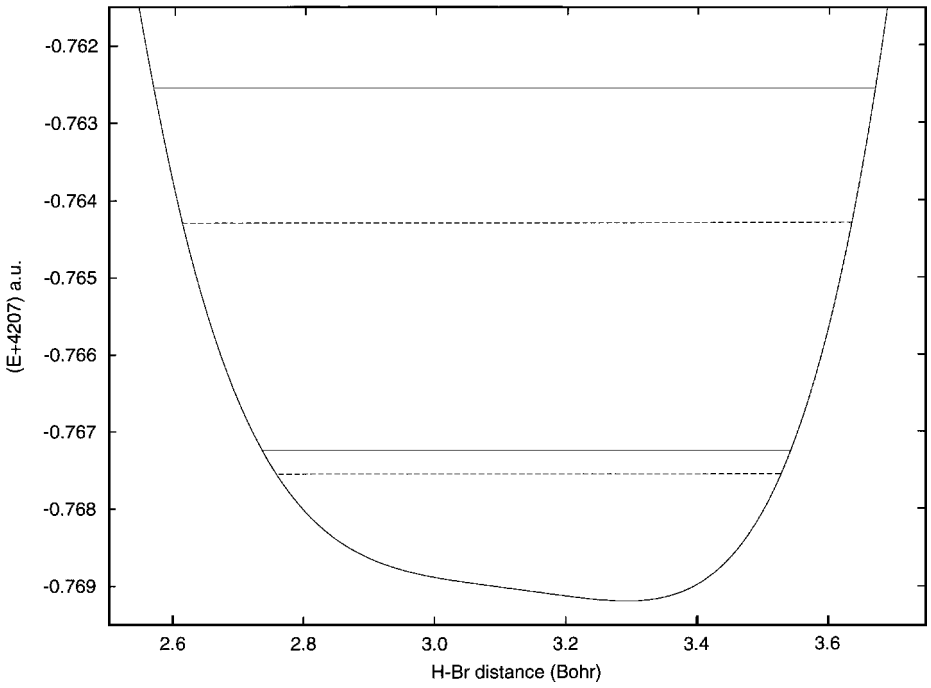

Figure 13. The potential energy and anharmonic vibrational energy levels (——) together with the harmonic levels (– – –) along the proton-stretching normal mode displacement vector for $BrH:NH_3$:3Ar, parameterized by the H–Br distance. (From Del Bene *et al.* (1997a), with permission.)

complexes are summarized in table 6. The complexes $XH:NH_3$:3Ar and $XH:NH_3$:3Ne have C_{3v} symmetry, with the inert-gas atoms staggered with respect to the ammonia hydrogen atoms. While the structures and spectra of the complexes of HF and HCl with NH_3 are not significantly changed by the presence of the rare-gas

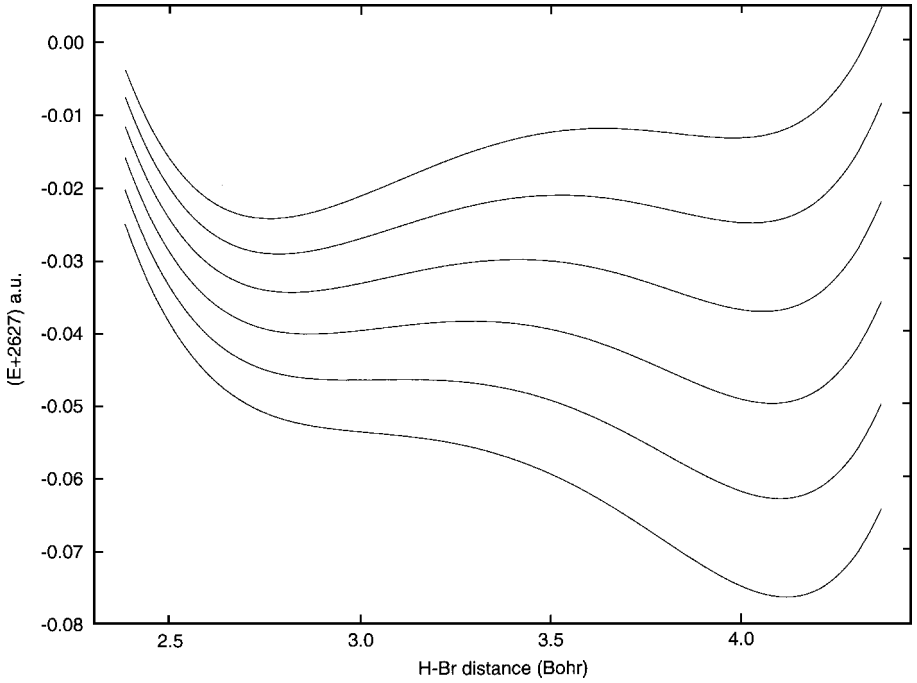

Figure 14. MP2/6-31 +G(d,p) potential energy curves along the normal coordinate for the proton-stretching mode in $BrH:NH_3$. Successive curves correspond to increasing field strength in the Br–H direction, beginning with zero field at the top and incrementing the field in steps of 0.0025 au. (From Del Bene *et al.* (1997a), with permission.)

atoms, these atoms have a dramatic effect on the $BrH:NH_3$ complex. Both $BrH:NH_3$:3Ne and $BrH:NH_3$:3Ar have equilibrium structures with proton-shared hydrogen bonds, and their computed harmonic spectra are typical of this hydrogen bond type. The computed proton-stretching frequencies for these complexes are 703 and 716 cm^{-1}, in very good agreement with the experimental argon matrix value of 729 cm^{-1}. How can the presence of a few inert-gas atoms have such a dramatic effect on the $BrH:NH_3$ complex? The answer to this question lies in the nature of the potential surface. As evident from figures 11 and 12, the $BrH:NH_3$ potential energy surface is relatively flat in the hydrogen-bonding region. The $BrH:NH_3$ structure with the traditional hydrogen bond is a polar complex, with a computed dipole moment of 4.79 D. The complex with the proton-shared hydrogen bond is even more polar, with a computed dipole moment of 8.40 D. It is not unreasonable to suggest that the argon atoms surrounding $BrH:NH_3$ can be polarized by this complex and they, in turn, can further polarize the complex, preferentially stabilizing the proton-shared structure. Because the traditional and proton-shared regions of the potential surface are energetically similar, what appears to be a dramatic matrix effect is not large from an energy point of view. However, it should be emphasized that the good agreement between the computed harmonic spectra of $BrH:NH_3$:3Ne and $BrH:NH_3$:3Ar and the experimental argon matrix spectrum of $BrH:NH_3$ is fortuitous. The potential curve corresponding to the normal coordinate displacement vector for the band at 716 cm^{-1} in $BrH:NH_3$:3Ar is shown in figure 13 and is obviously anharmonic. The anharmonic one-dimensional proton-stretching frequency obtained from this curve is 1030 cm^{-1}, 314 cm^{-1} greater than the harmonic frequency.

Some insight into the effect of the presence of inert-gas atoms can be obtained by examining figure 14. Plotted in this figure are MP2/6-31 +G(d, p) potential curves for proton motion obtained from the normal coordinate displacement vector for the band at 2006 cm^{-1} in $BrH:NH_3$ as a function of external electric field strength applied in the Br–H direction (Del Bene *et al.* 1997a). It is apparent from figure 14 that the introduction of a field has both qualitative and quantitative effects, converting the double minimum to a single minimum, and stabilizing the proton-shared structure relative to the structure with a traditional hydrogen bond. Even the weakest field of 0.0025 au alters the relative stabilities of the two complexes and, as the field strength increases, the single minimum moves toward a proton-shared and then an ion-pair structure.

6.4. *Charged complexes*

The discussion of the structures and vibrational spectra of hydrogen-bonded complexes has been limited thus far to neutral complexes. Hydrogen bonding may also occur between a charged and a neutral species, giving rise to a complex that bears a net positive or negative charge. The structures of charged complexes usually have short intermolecular distances but, from a structural point of view, can have either traditional or proton-shared hydrogen bonds. For example, the computed MP2/6-31 +G(d, p) structure of the complex $NH_4^+:H_2O$ has a traditional N–H···O hydrogen bond with an intermolecular distance of 2.725 Å, and a harmonic spectrum typical of this structure type with a strong band above 3000 cm^{-1}. (By comparison, the pyrrole:H_2O complex also has a traditional hydrogen bond, but the computed intermolecular distance is 2.977 Å at the same level of theory. The N–H stretching band is typical for a complex with a traditional hydrogen bond, occurring at 3674 cm^{-1}).

In contrast, the complex $O_2H_5^+$ is stabilized by a symmetric proton-shared O···H···O hydrogen bond, with a computed MP2/6-31 +G(d, p) intermolecular distance of 2.385 Å, and a harmonic spectrum that exhibits several strong bands below 1800 cm^{-1}. (By comparison, $(H_2O)_2$ has a traditional O–H···O hydrogen bond with an O–O distance of 2.914 Å. The hydrogen-bonded proton stretching frequency is 3788 cm^{-1} at the same level of theory.) Ojamäe *et al.* (1995) have computed harmonic frequencies and anharmonic proton- and dimer-stretching frequencies in $O_2H_5^+$ based on MP2/aug´-cc-pVTZ energies using a DVR scheme. The computed O–O distance is 2.396 Å, and the harmonic frequency for the proton stretch is 983 cm^{-1}. The anharmonic stretching frequencies obtained from the one- and two-dimensional treatments are higher than the harmonic frequency, at 1623 and 1275 cm^{-1} respectively. The inadequacy of the harmonic treatment is again evident in this complex.

6.5. *The XHX^- anions*

The bihalide ions XHX^- (X = F, Cl or Br) are the simplest hydrogen-bonded complexes that are stabilized by proton-shared hydrogen bonds. Their small size and high symmetry make feasible the calculation of potential energy surfaces at very accurate levels of theory. The structures of these complexes and the computed harmonic frequencies for the symmetric (ν_1, heavy atom) and asymmetric (ν_3, proton) stretching modes and the bending (ν_2) mode are reported in table 7 (Del Bene and Jordan 1999). These calculations were carried out at MP2/6-31 +G(d, p), MP2/aug´-cc-pVTZ, CCSD/aug´-cc-pVTZ and CCSD(T)/aug´-cc-pVTZ levels of theory. In almost all cases, the optimized geometry was found to have $D_{\infty h}$ symmetry. (The exceptions are $ClHCl^-$ and $BrHBr^-$ which have equilibrium structures of $C_{\infty v}$

Table 7. Calculated equilibrium geometries and harmonic frequencies for the symmetric stretch (ν_1), the bend (ν_2) and the asymmetric stretch (ν_3) of complexes XHX^-.

XHX^-	Symmetry	Level of theory	X–H (Å)	ν_1 (cm^{-1})	ν_2 (cm^{-1})	ν_3 (cm^{-1})
FHF^-	$D_{\infty h}$	MP2/6-31 +G(d, p)	1.150	635	1380	1299
	$D_{\infty h}$	MP2/aug´-cc-pVTZ	1.114	633	1334	1280
	$D_{\infty h}$	CCSD/aug´-cc-pVTZ	1.137	650	1368	1205
	$D_{\infty h}$	CCSD(T)/aug´-cc-pVTZ	1.141	640	1347	1244
$ClHCl^-$	$D_{\infty h}$	MP2/6-31 +G(d, p)	1.550	353	893	108
	$D_{\infty h}$	MP2/aug´-cc-pVTZ	1.555	345	843	629
	$C_{\infty v}$	CCSD/aug´-cc-pVTZ	1.470, 1.668	174	828	761
	$D_{\infty h}$	CCSD(T)/aug´-cc-pVTZ	1.556	344	831	426
$BrHBr^-$	$D_{\infty h}$	MP2/6-31 +G(d, p)	1.710	209	767	575
	$D_{\infty h}$	MP2/aug´-cc-pVTZ	1.695	209	743	646
	$C_{\infty v}$	CCSD/aug´-cc-pVTZ	1.613, 1.809	114	731	636
	$D_{\infty h}$	CCSD(T)/aug´-cc-pVTZ	1.703	206	767	354

symmetry at CCSD/aug´-cc-pVTZ. However, the barrier between the two equilibrium structures is negligible.) Since the nature of the XHX^- potential energy surfaces in the region of the global minimum varies considerably with the level of theory used, minor very-low-energy features can have a significant effect on calculated harmonic frequencies, as evident from table 7. Because an anharmonic two-dimensional treatment vibrationally averages over any low-energy features, the anharmonic symmetric and asymmetric stretching frequencies are not as sensitive to the level of theory used, as shown in table 8. Even the lowest level of theory considered (MP2/6-31 +G(d, p)) provides a qualitatively correct, and surprisingly accurate, description of the stretching modes in these anions. The anharmonic vibrational frequencies for the symmetric and asymmetric stretching modes discussed below are those obtained at the highest level of theory, CCSD(T)/aug´-cc-pVTZ.

6.5.1. *FHF^- and FDF^-*

The CCSD(T)/aug´-cc-pVTZ symmetric stretching frequency for FHF^- is 595 cm^{-1}, in agreement with the experimental gas-phase value of 583 cm^{-1} (Kawaguchi and Hirota 1987). In a matrix the frequency of the symmetric stretching band is often not directly observable, but is estimated as the algebraic difference between the combination band ($\nu_1 + \nu_3$) and the fundamental frequency for the asymmetric stretch (ν_3). The experimental gas-phase frequency of the symmetric stretch in FHF^- obtained as the algebraic difference between the observed combination band ($\nu_1 + \nu_3$) and the observed ν_3 fundamental, that is ($\nu_1 + \nu_3$) $- \nu_3$, is 516 cm^{-1} (Kawaguchi and Hirota 1987) compared with 531 cm^{-1} at CCSD(T)/aug´-cc-pVTZ. These values are lower than those obtained for ν_1 directly, that is the ν_1 stretching frequency is dependent on the observed ν_3 manifold, an indication of the coupling between the symmetric and asymmetric stretching coordinates on the potential energy surface.

While the computed harmonic frequencies for the asymmetric stretch in FHF^- are too low relative to experiment, the anharmonic frequencies are too high. The CCSD(T)/aug´-cc-pVTZ frequency is 1476 cm^{-1}, 145 cm^{-1} greater than the experimental gas-phase value of 1331 cm^{-1} (Kawaguchi and Hirota 1987). Matrix values

Table 8. Expectation values for the X–H distance in the ground vibrational state and anharmonic and experimental frequencies for the symmetric (ν_1) and asymmetric (ν_3) stretches and combination band ($\nu_1 + \nu_3$) $- \nu_3$ for complexes XHX^-.

XHX^-	Method	$\langle X-H \rangle$ (Å)	ν_1 (cm^{-1})	ν_3 (cm^{-1})	($\nu_1 + \nu_3$) $- \nu_3$ (cm^{-1})
FHF^-	MP2/6-31 +G(d, p)	1.167	593	1499	
	MP2/aug´-cc-pVTZ	1.162	589	1485	527
	CCSD/aug´-cc-pVTZ	1.155	603	1461	535
	CCSD(T)/aug´-cc-pVTZ	1.158	595	1476	531
Experiment	Gas phase[a]		583	1331	516
	Ne matrix[b]			1379	
	Ar matrix[b, c]			1377	
	Ar matrix[d]			1364	
$ClHCl^-$	MP2/6-31 +G(d, p)	1.575	307	697	253
	MP2/aug´-cc-pVTZ	1.576	317	881	278
	CCSD/aug´-cc-pVTZ	1.584	304	697	261
	CCSD(T)/aug´-cc-pVTZ	1.584	308	776	267
Experiment	Gas phase[e]		318	723	
	Ar matrix[f–i]			696	259
	Kr matrix[f]			663	253
	Xe matrix[f]			644	249
$BrHBr^-$	MP2/6-31 +G(d, p)	1.729	195	785	168
	MP2/aug´-cc-pVTZ	1.715	195	846	173
	CCSD/aug´-cc-pVTZ	1.726	186	649	160
	CCSD(T)/aug´-cc-pVTZ	1.726	188	731	165
Experiment	Ar matrix[j, k]			728	164
	Kr matrix[f]			687	159
	Xe matrix[f]			646	152

[a] From Kawaguchi and Hirota (1987).
[b] From Hunt and Andrews (1987).
[c] From McDonald and Andrews (1979).
[d] From Ault (1979).
[e] From Kawaguchi (1988).
[f] From Räsänen *et al.* (1993).
[g] From Noble and Pimentel (1968).
[h] From Milligan and Jacox (1970).
[i] From Wright *et al.* (1976).
[j] From Bondybey *et al.* (1971).
[k] From Milligan and Jacox (1971).

for the asymmetric stretch vary from 1379 cm^{-1} in neon to 1377 and 1364 cm^{-1} in argon. There may be several factors responsible for the differences between the computed and the experimental gas-phase values, but one that must be considered is the neglect of coupling between bending and stretching modes in the two-dimensional treatment. This coupling will be the subject of future studies.

Anharmonic effects on the vibrational frequencies may be understood in terms of the profiles of the potential energy surface taken along the symmetric and asymmetric stretching coordinates. These are illustrated by the CCSD(T)/aug´-cc-pVTZ plots shown in figure 15. It is apparent that the asymmetric stretch is dominated by the repulsive nature of the potential wall. Indeed, the anharmonic calculations show that the spacing between asymmetric stretch eigenvalues increases with increasing energy.

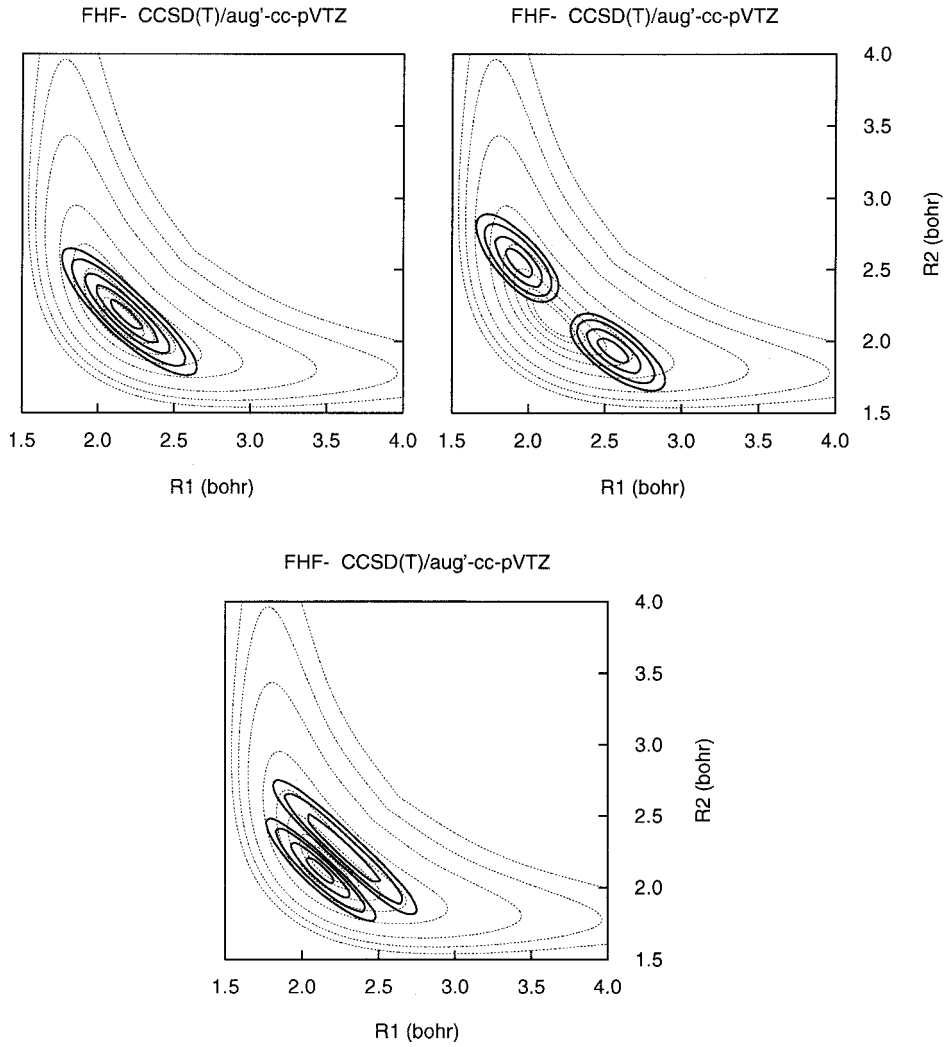

Figure 15. The CCSD(T)/aug´-cc-pVTZ potential surface for FHF^-. The square of the wavefunction for the ground vibrational state (top left) and for the v = 1 excited states of the symmetric (top right) and asymmetric (bottom) stretches are shown superimposed on the surface. The contours are at 0.0005, 0.001, 0.0025, 0.005, 0.01, 0.02, 0.03 and 0.04 au above the global minimum energy.

Thus, the anharmonicity constant c_{33} is found to be positive. The symmetric stretch, however, exhibits more typical behaviour with c_{11} negative. The relative insensitivity of the anharmonic asymmetric stretching frequency to the level of theory can be rationalized in terms of figure 15. Although the nature of the potential in the vicinity of the equilibrium structure depends markedly on the level of theory used, the location and curvature of the repulsive walls in the potential surface at short X–H bond lengths are much less sensitive. The potential surfaces for $ClHCl^-$ and $BrHBr^-$ are qualitatively similar to figure 15.

The computed and experimental anharmonic stretching frequencies for the deuterium-substituted complex FDF^- are given in table 9. Deuterium substitution has only a small effect on the symmetric stretching frequency as the dominant motion is

Table 9. Experimental and computed CCSD(T)/aug´-cc-pVTZ anharmonic frequencies for the symmetric (ν_1) and asymmetric (ν_3) stretches and the combination band $(\nu_1 + \nu_3) - \nu_3$ in the deuterated species XDX^-.

XDX^-	Method	ν_1 (cm^{-1})	ν_3 (cm^{-1})	$(\nu_1 + \nu_3) - \nu_3$ (cm^{-1})
FDF^-	CCSD(T)/aug´-cc-pVTZ	601	1023	546
Experiment	Ar matrix[a,b]		965	
	Ar matrix[c]		969	
$ClDCl^-$	CCSD(T)/aug´-cc-pVTZ	308	507	271
Experiment	Ar matrix[d–f]		463	267
	Kr matrix[g]		438	255
$BrDBr^-$	CCSD(T)/aug´-cc-pVTZ	189	479	168
Experiment	Ar matrix[h,i]		498	170
	Kr matrix[g]		466	164
	Xe matrix[g]		435	158

[a] From Hunt and Andrews (1987).
[b] From McDonald and Andrews (1979).
[c] From Ault (1979).
[d] From Noble and Pimentel (1968).
[e] From Milligan and Jacox (1970).
[f] From Wright *et al.* (1976).
[g] From Räsänen *et al.* (1993).
[h] From Bondybey *et al.* (1971).
[i] From Milligan and Jacox (1971).

that of the heavy atoms, but leads to a significant decrease in the asymmetric stretching frequency, as expected. The experimental argon matrix asymmetric stretching frequency of FDF^- is 414 cm^{-1} lower than that of FHF^-. The computed CCSD(T)/aug´-cc-pVTZ lowering is 453 cm^{-1}. For the asymmetric stretch the computed ratio $\nu_1(FHF^-)/\nu_1(FDF^-)$ of 1.44 is slightly larger than the harmonic value of 1.414, and in agreement with the experimental argon matrix ratio of 1.42.

6.5.2. *ClHCl⁻ and ClDCl⁻*

The gas-phase frequency of 318 cm^{-1} for the symmetric stretch in $ClHCl^-$ was computed by Kawaguchi (1988) from the observed centrifugal distortion constant. This value is in agreement with the computed CCSD(T)/aug´-cc-pVTZ frequency of 308 cm^{-1}. The reported experimental ν_1 stretching frequencies obtained in inert matrices were not observed directly, but again obtained from the algebraic difference $(\nu_1 + \nu_3) - \nu_3$. Experimentally, these frequencies range from 249 to 259 cm^{-1} and are significantly lower than the gas-phase value obtained directly for ν_1. When the symmetric stretching frequency is computed in the same way, the CCSD(T)/aug´-cc-pVTZ value is 267 cm^{-1}. The anharmonicity of the potential surface is evident from these results. The computed CCSD(T)/aug´-cc-pVTZ symmetric stretching frequency ν_3 is 776 cm^{-1}, about 50 cm^{-1} higher than the experimental gas-phase value of 723 cm^{-1} (Kawaguchi 1988). Botschwina *et al.* (1988) have computed similar symmetric and asymmetric frequencies of 308 and 768 cm^{-1} using the CEPA-1 method.

Table 9 reports the frequencies for the symmetric and asymmetric stretches in $ClDCl^-$. The computed CCSD(T)/aug´-cc-pVTZ frequency for the asymmetric stretch is 507 cm^{-1}, 269 cm^{-1} lower than the computed value for $ClHCl^-$. The corresponding

difference obtained from argon matrix measurements is 232 cm^{-1}. The computed CCSD(T)/aug´-cc-pVTZ ratio $\nu_1(ClHCl^-)/\nu_1(ClDCl^-)$ is 1.53, in good agreement with the experimental ratio of 1.50, and much larger than the expected harmonic ratio of 1.414.

6.5.3. *$BrHBr^-$ and $BrDBr^-$*

The computed and experimental anharmonic frequencies for the symmetric and asymmetric stretches in $BrHBr^-$ are reported in table 8. The CCSD(T)/aug´-cc-pVTZ frequency for the symmetric stretch is 188 cm^{-1}. The gas-phase frequency has not been observed but has again been estimated in inert matrices as $(\nu_1 + \nu_3) - \nu_3$ and found to range from 152 to 164 cm^{-1}. The frequency calculated in the same way as $(\nu_1 + \nu_3) - \nu_3$ is 165 cm^{-1}, in agreement with experiment. The experimental gas-phase frequency for the asymmetric stretch is not available, but the inert matrix values range from 646 to 728 cm^{-1}. The CCSD(T)/aug´-cc-pVTZ frequency for the asymmetric stretch is 731 cm^{-1}.

The computed CCSD(T)/aug´-cc-pVTZ frequency for the asymmetric stretch in $BrDBr^-$ is 479 cm^{-1}, similar to the inert matrix values which range from 435 to 498 cm^{-1}. The observed isotopic shift ratio $\nu_1(BrHBr^-)/\nu_1(BrDBr^-)$ is 1.49 experimentally in an argon matrix, and 1.53 at CCSD(T)/aug´-cc-pVTZ, both values clearly exceeding the harmonic ratio.

7. Concluding comments

Is it possible to predict the nature of the experimental spectrum of a hydrogen-bonded complex based on the computed structure of this complex and its computed harmonic spectrum? Can the experimental IR spectrum be used to infer the type of hydrogen bond present? Can the harmonic approximation provide reliable proton-stretching frequency shifts in hydrogen-bonded complexes? These questions cannot be answered with a simple 'yes' or 'no'. From studies carried out thus far, there does appear to be a relationship between the computed structure of a hydrogen-bonded complex and its computed harmonic spectrum. Complexes with traditional hydrogen bonds have computed spectra typical of this hydrogen bond type, while those with proton-shared hydrogen bonds again have typical computed spectra characterized by strong low-frequency proton-stretching bands. However, structure alone is not sufficient to determine the IR spectrum of a hydrogen-bonded complex. IR spectroscopy is a very sensitive probe of hydrogen bonding, but it is a probe not only of the potential well in which the equilibrium structure resides, but also of the potential energy surface accessible in either the $v = 0$ or the $v = 1$ vibrational state of the proton-stretching mode. If a complex with a traditional hydrogen bond resides in a deep potential well so that both the $v = 0$ and the $v = 1$ vibrational states are confined to the well, there will be a correlation between structure type and spectrum, and this correlation will be seen both experimentally (between the gas-phase structure and the IR spectrum obtained in an argon matrix) and theoretically (from the computed *ab initio* structure and the harmonic IR spectrum, provided of course that an appropriate level of theory is used for the calculations). In this case, the computed frequency shift of the A–H band upon formation of the A–H···B hydrogen bond should be in reasonable agreement with the experimental shift. On the other hand, if the potential well for a complex stabilized by a traditional hydrogen bond is broad and relatively flat, or if a second region of the surface is accessible in either the $v = 0$ or the $v = 1$ vibrational state of the proton-stretching vibration, both experiment and theory may

give conflicting descriptions of the structure and spectrum of the complex. A harmonic treatment of the proton-stretching vibration cannot describe the anharmonicity inherent in the potential energy surface. In these complexes, matrix effects may also have increased importance, since the matrix will preferentially stabilize the more polar structure with a proton-shared hydrogen bond.

In complexes stabilized by proton-shared hydrogen bonds, it appears that both the experimental and the computed harmonic spectra will exhibit strong low-frequency bands associated with the proton-stretching vibration but, inevitably, there will be differences between the experimental and the computed frequencies and intensities of these bands. The harmonic approximation again fails because of the inability of a parabolic curve to describe adequately the flatness of the potential surface in the hydrogen-bonding region. If there is apparent agreement between the experimental spectrum and the computed harmonic spectrum of a complex with a proton-shared hydrogen bond, this agreement must be fortuitous. Anharmonicity effects will also be evident in the experimental spectra of these complexes from the appearance of combination bands and from the effects of deuterium substitution. Computed anharmonic frequencies for both fundamental and combination bands are needed to understand and reproduce qualitatively the most important features of the experimental spectra of these hydrogen-bonded complexes.

Acknowledgements

This work was supported by National Science Foundation research grants CHE-9505888 and 9873815. The calculations were performed on computing facilities at the Ohio Supercomputer Center and at the University of Cambridge.

References

Anderson, J. B., 1975, *J. chem. Phys.*, **63**, 1499; 1976, *ibid.*, **65**, 4121; 1980, *J. chem. Phys.*, **73**, 3897.

Antikainen, J., Friesner, R., and Leforestier, C., 1995, *J. chem. Phys.*, **102**, 1270.

Ault, B. S., 1979, *J. phys. Chem.*, **83**, 837.

Bačić, Z., and Light, J. C., 1989, *An. Rev. phys. Chem.*, **40**, 469.

Bačić, Z., Watt, D., and Light, J. C., 1988, *J. chem. Phys.*, **89**, 947.

Ballard, L., and Henderson, G. J., 1991, *Phys. Chem.*, **95**, 660.

Barnes, A. J., 1983, *J. molec. Struct.*, **100**, 259.

Barnes, A. J., Beech, T. R., and Mielke, Z., 1984, *J. chem. Soc., Faraday Trans.* II, **80**, 455.

Barnes, A. J., and Legon, A. C., 1998, *J. molec. Struct.*, **448**, 101.

Bartlett, R. J., 1989, *J. phys. Chem.*, **93**, 1697.

Bartlett, R. J., Cole, S. J., Purvis, G. D., Ermler, W. C., Hsieh, H. C. and Shavitt, I., 1988, *J. chem. Phys.*, **87**, 6579.

Bartlett, R. J., and Silver, D. M., 1975, *J. chem. Phys.*, **62**, 3258.

Bartlett, R. J., and Stanton, J. F., 1994, *Reviews of Computational Chemistry*, Vol. V., edited by K. B. Lipkowitz and D. B. Boyd (New York: VCH), pp. 65–169.

Bartlett, R. J., Stanton, J. F., and Watts, J. D., 1991, *Advances in Molecular Vibrations and Collision Dynamics*, Vol. 1B, edited by J. Bowman. (Greenwich, Connecticut: JAI Press), pp. 139–167.

Bartlett, R. J., Watts, J. D., Kucharski, S. A., and Noga, J., 1990, *Chem. Phys. Lett.*, **165**, 513.

Bernu, B., Ceperley, D. M., and Lester, W. A., 1990, *J. chem. Phys.*, **93**, 552.

Blume, D., Lewerenz, M., Niyaz, P., and Whaley, K. B., 1997a, *Phys. Rev. E*, **55**, 3664.

Blume, D., Lewerenz, M., and Whaley, K. B., 1997b, *J. chem. Phys.*, **107**, 9067.

Bock, C. W., Trachtman, M., and George, P., 1980, *J. molec. Spectrosc.*, **84**, 256.

BONDYBEY, V., PIMENTEL, G. C., and NOBLE, P. N., 1971, *J. chem. Phys.*, **55**, 540.†
BOTSCHWINA, P., 1979, *Chem. Phys.*, **40**, 33.
BOTSCHWINA, P., and SEBALS, P., 1983, *J. molec. Spectrosc.*, **100**, 1.
BOTSCHWINA, P., SEBALS, P., and BURMEISTER, R., 1988, *J. chem. Phys.*, **88**, 5246.
BOWMAN, J. M., 1978, *J. chem. Phys.*, **68**, 608; 1986, *Accts chem. Res.*, **19**, 202.
BOWMAN, J. M., ZUNIGA, J., and WIERZBICKI, A., 1989, *J. chem. Phys.*, **90**, 2708.
BRAMLEY, M. J., and CARRINGTON, T., JR, 1993, *J. chem. Phys.*, **99**, 8519.
CARTER, S., and HANDY, N. C., 1982, *Molec. Phys.*, **47**, 1445; 1986, *ibid.*, **57**, 175.
CARTER, S., HANDY, N. C., and PINNAVAIA, N., 1995, *Chem. Phys. Lett.*, **240**, 400.
CEPERLEY, D. M., and ALDER, B. J., 1981, *Physica* B, **108**, 875.
CEPERLEY, D. M., and BERNU, B., 1988, *J. chem. Phys.*, **89**, 6316.
CHANG, J., MOISEYEV, N., and WYATT, R. E., 1986, *J. chem. Phys.*, **84**, 4997.
CHEN, R., and GUO, H., 1996, *J. chem. Phys.*, **105**, 1331.
CLARK, T., CHANDRASEKHAR, J., SPITZNAGEL, G. W., and SCHLEYER, P. v. R., 1983, *J. comput. Chem.*, **4**, 294.
CLARY, D. C., GREGORY, J. K., JORDAN, M. J. T., and KAUPPI, E., 1997, *J. chem. Soc., Faraday Trans.*, **93**, 747.
COKER, D. F., and WATTS, R. O., 1986, *Molec. Phys.*, **58**, 1113; 1987, *J. phys. Chem.*, **91**, 2513.
COLLINS, M. A., and PARSONS, D. F., 1993, *J. chem. Phys.*, **99**, 6756.
COOKE, S. A., CORLETT, G. K., LISTER, D. G., and LEGON, A. C., 1998, *J. chem. Soc., Faraday Trans.*, **94**, 837.
CSASZAR, A. G., 1992, *J. Phys. Chem.*, **96**, 7898; 1994, *ibid.*, **98**, 8823.
CSASZAR, A. G., and MILLS, I. M., 1997, *Spectrochim. Acta* A, **53**, 1001.
CULLUM, J. K., and WILLOUGHBY, R. A., 1985, *Lanczos Algorithms for Large Symmetric Eigenvalue Computations*, (Boston, Massachusetts: Birkhäuser).
DEL BENE, J., and POPLE, J. A., 1970, *J. chem. Phys.*, **52**, 4858.
DEL BENE, J. E., 1992, *Int. J. quant. Chem., quant. Chem. Symp.*, **26**, 527; 1998, *Encyclopedia of Computational Chemistry*, Vol. 2, edited by P. v. R. Schleyer, N. L. Allinger, T. Clark, J. Gasteiger, P. A. Kollman, H. F. Schaefer, III and P. R. Schreiner (Chichester, UK: Wiley), pp. 1263–1271.
DEL BENE, J. E., and JORDAN, M. J. T., 1998, *J. chem. Phys.*, **108**, 3205; 1999, *Spectrochim. Acta* A, **55**, 719.
DEL BENE, J. E., JORDAN, M. J. T., GILL, P. M. W., and BUCKINGHAM, A. D., 1997a, *Molec. Phys.*, **93**, 429.
DEL BENE, J. E., PERSON, W. B., and SZCZEPANIAK, K., 1995, *J. phys. Chem.*, **99**, 10705; 1996, *Molec. Phys.*, **89**, 47.
DEL BENE, J. E., and SHAVITT, I., 1997, *Molecular Interactions*, edited by S. Scheiner, (Chichester, West Sussex: Wiley), pp. 157–179.
DEL BENE, J. E., SZCZEPANIAK, K., CHABRIAR, P., and PERSON, W. B., 1997b, *Chem. Phys. Lett.*, **264**, 109; 1997c, *J. phys. Chem.*, **101**, 4481.
DUNHAM, J. L., 1932, *Phys. Rev.*, **41**, 721.
DUNN, K. M., BOGGS, J. E., and PULAY, P., 1986, *J. chem. Phys.*, **85**, 5838.
DUNNING, T. J., JR, 1989, *J. chem. Phys.*, **90**, 1007.
DYKE, T. R., HOWARD, B. J., and KLEMPERER, W., 1969, *J. chem. Phys.*, **56**, 2442.
DYKE, T. R., MACK, K. M., and MUENTER, J. S., 1977, *J. chem. Phys.*, **66**, 498.
DYKE, T. R., and MUENTER, J. S., 1973, *J. chem. Phys.*, **59**, 3125.
DYKSTRA, C. E., AUGSPURGER, J. D., KIRTMAN, B., and MALIK, D. J., 1990, *Reviews of Computational Chemistry*, Vol. 1, edited by K. B. Kipkowitz and D. B. Boyd (New York: VCH), pp. 83–118.
ECHAVE, J., and CLARY, D. C., 1992, *Chem. Phys. Lett.*, **190**, 225.
ENGDAHL, A., and NELANDER, B. J., 1989, *Molec. Struct.*, **193**, 101.
FEIT, M. D., FLECK, J. A., and STEIGER, A., 1982, *J. comput. Phys.*, **47**, 412.
FELLER, D., GLENDENING, E. D., KENDALL, R. A., and PETERSON, K. A., 1994, *J. chem. Phys.*, **100**, 4981.
FOGARASI, G., and PULAY, P., 1984, *A. Rev. phys. Chem.*, **35**, 191.
FREY, J. G., and HOWARD, B. J., 1985, *Chem. Phys.*, **99**, 427.

† Frequencies originally assigned to the neutral species have been reassigned to the ions by Milligan and Jacox (1971).

FRISCH, M. J., DEL BENE, J. E., BINKLEY, J. S., and SCHAEFER, H. F., III, 1986, *J. chem. Phys.*, **84**, 2279.
GAUSS, J., and CREMER, D., 1992, *Adv. quant. Chem.*, **23**, 206.
GAW, J. F., and HANDY, N. C., 1985, *Chem. Phys. Lett.*, **121**, 321; 1986, *ibid.*, **128**, 182.
GAW, J. F., HANDY, N. C., PALMIERI, P., and DEGLI ESPOSTI, A., 1988, *J. chem. Phys.*, **89**, 959.
GAW, J. F., WILLETTS, A., GREEN, W. H., and HANDY, N. C., 1991, *Advances in Molecular Vibrations and Collision Dynamics*, Vol. 1C, edited by J. M. Bowman (Greenwich, Connecticut: JAI Press), pp. 169–185.
GREGORY, J. K., 1998, *Chem. Phys. Lett.*, **282**, 147.
GREGORY, J. K., and CLARY, D. C., 1995, *J. chem. Phys.*, **192**, 7817; 1996, *J. phys. Chem.*, **100**, 18014.
GROZDANOV, T. P., MANDELSHTAM, V. A., and TAYLOR, H. S., 1995, *J. chem. Phys.*, **103**, 7990.
HANDY, N. C., 1987, *Molec. Phys.*, **61**, 207; 1989, *Int. Rev. phys. Chem.*, **8**, 275.
HANKINS, D., MOSKOWITZ, J. W., and STILLINGER, F. H., 1970, *Chem. Phys. Lett.*, **4**, 527.
HARIHARAN, P. C., and POPLE, J. A., 1973, *Theor. chim. Acta*, **28**, 213.
HARTKE, B., and WERNER, H. J., 1997, *Chem. Phys. Lett.*, **280**, 430.
HEHRE, W. J., DITCHFIELD, R., and POPLE, J. A., 1972, *J. chem. Phys.*, **56**, 2257.
HEHRE, W. J., RADOM, L., SCHLEYER, P. v. R., and POPLE, J. A., 1986, *Ab Initio Molecular Orbital Theory* (New York: Wiley).
HOY, A. R., MILLS, I. M., and STREY, G., 1972, *Molec. Phys.*, **24**, 1265.
HUANG, Y., KOURI, D. J., and HOFFMAN, D. K., 1994, *J. chem. Phys.*, **101**, 10493.
HUANG, Y., LYENGAR, S. S., KOURI, D. J., and HOFFMAN, D. K., 1996, *J. chem. Phys.*, **105**, 927.
HUNT, R. D., and ANDREWS, L., 1987, *J. chem. Phys.*, **87**, 6819.
ISHTWAN, J., and COLLINS, M. A., 1991, *J. chem. Phys.*, **94**, 7084.
IUNG, C., and LEFORESTIER, C., 1992, *J. chem. Phys.*, **97**, 2481; 1995, *Ibid.*, **102**, 8453.
JOHNSON, B. R., and REINHARDT, W. P., 1986, *J. chem. Phys.*, **85**, 4538.
JOHNSON, G. L., and ANDREWS, L., 1982, *J. Am. chem. Soc.*, **104**, 3043.
JORDAN, M. J. T., THOMSON, K. C., and COLLINS, M. A., 1995, *J. chem. Phys.*, **102**, 5647.
JUCKS, K. W., and MILLER, R. E., 1987, *J. chem. Phys.*, **86**, 6637.
KAWAGUCHI, K., 1988, *J. chem. Phys.*, **88**, 4186.
KAWAGUCHI, K., and HIROTA, E., *J. chem. Phys.*, **87**, 6838.
KENDALL, R. A., DUNNING, T. H., JR, and HARRISON, R. J., 1992, *J. chem. Phys.*, **96**, 1358.
KIM, J., LEE, J. Y., LEE, S., MHIN, B. J., and KIM, K. S., 1995, *J. chem. Phys.* **102**, 310.
KOLLMAN, P. A., and ALLEN, L. C., 1969, *J. chem. Phys.*, **51**, 3286; 1972, *Chem. Rev.*, **72**, 283.
KONDO, S., KOGA, Y., and NAKANGA, T., 1984, *J. chem. Phys.*, **81**, 1951.
KONO, H., 1993, *Chem. Phys. Lett.*, **214**, 137.
KOPUT, J., and CARTER, S., 1997, *Spectrochim. Acta* A, **53**, 1091.
KOURI, D. J., ZHU, W., PARKER, G. A., and HOFFMAN, D. K., 1995, *Chem. Phys. Lett.*, **238**, 395.
KYRO, E. K., SHOJA-CHAGHERVAND, P., MCMILLAN, K., ELIADES M., DANZEISER, D., and BEVAN, J. W., 1983, *J. chem. Phys.*, **79**, 28.
LANCZOS, C., 1950, *J. Res. natn. Bur. Stand.*, **45**, 255.
LATAJKA, Z., SCHEINER, S., and RATAJCZAK, H., 1987, *Chem. Phys. Lett.*, **135**, 367; 1992, *Chem. Phys.*, **166**, 85.
LATAJKA, Z., SUKAI, S., MOROKUMA, K., and RATAJCZAK, H., 1984, *Chem. Phys. Lett.*, **110**, 464.
LEE, T. J. (editor), 1997, *Spectrochimica Acta* A, **53**, No. 8.
LEGON, A. C., 1993, *Chem. Soc. Rev.*, **22**, 153.
LEGON, A. C., and MILLEN, D. J., 1986, *Chem. Rev.*, **86**, 635; 1988, *Proc. R. Soc.* A, **417**, 21; 1992, *Chem. Soc. Rev.*, **21**, 71.
LEGON, A. C., MILLEN, D. J., and NORTH, H. M., 1987, *J. chem. Phys.*, **86**, 2530.
LEGON, A. C., SOPER, P. D., and FLYGARE, W. H., 1981, *J. chem. Phys.*, **74**, 4944.
LEROY, R. J., and CARLEY, J. S., 1980, *Adv. chem. Phys.*, **42**, 353.
LIAS, S. G., BARTMESS, J. E., LIEBMAN, J. F., HOLMES, J. L., LEVIN, R. D., and MALLARD, W. G., 1988, *J. Phys. Chem. Ref. Data*, Suppl. 1.
MACDONALD, J. F. L., 1933, *Phys. Rev.*, **43**, 830.
MAHAPATRA, S., VETTER, R., ZUHRT, C., NGUYEN, H. T., RITSCHEL, T., and ZULICKE, L., 1998, *Chem. Phys. Lett.*, **285**, 41.
MANDELSHTAM, V. A., GROZDANOV, T. P., and TAYLOR, H. S., 1995, *J. chem. Phys.*, **103**, 10074.
MANDELSHTAM, V. A., and TAYLOR, H. S., 1995, *J. chem. Phys.*, **103**, 2903.

MANDELSHTAM, V. A., TAYLOR, H. S., and MILLER, W. H., 1996, *J. chem. Phys.*, **105**, 496.
MCDONALD, S. A., and ANDREWS, L., 1979, *J. chem. Phys.*, **70**, 3134.
MEYER, W., BOTSHWINA, P., and BURTON, P., 1986, *J. chem. Phys.*, **84**, 891.
MILLER, R. E., COKER, D. F., and WATTS, R. O., 1985, *J. chem. Phys.*, **82**, 3554.
MILLS, I. M., 1972, *Molecular Spectroscopy: Modern Research*, Vol. I, edited by K. N. Rao and C. W. Mathews (New York: Academic Press); pp. 115–140, 1974, *Theoretical Chemistry*, Vol. I, edited by R. N. Dixon (London: Chemical Society), pp. 110–159.
MILLIGAN, D. E., and JACOX, M. E., 1970, *J. chem. Phys.*, **53**, 2034; 1971, *ibid.*, **55**, 2550.
MOROKUMA, K., and PEDERSEN, L., 1968, *J. chem. Phys.*, **48**, 3275.
MOROKUMA, K., and WINICK, J., 1970, *J. chem. Phys.*, **52**, 1301.
MURRELL, J. N., CARTER, S., FARANTOS, S. C., HUXLEY, P., and VARANDAS, A. J. C., 1984, *Molecular Potential Energy Functions* (Chichester, West Sussex: Wiley).
NEUHAUSER, D., 1990, *J. chem. Phys.*, **93**, 2611; 1994, *J. chem. Phys.*, **100**, 5076.
NOBLE, P. N., and PIMENTEL, G. C., 1968, *J. chem. Phys.*, **49**, 3165.†
ODUTOLA, J. A., VISWANATHAN, R., and DYKE, T. R., 1979, *J. Am. chem. Soc.*, **101**, 4787.
OJAMÄE, L., SHAVITT, I., and SINGER, J., 1995, *Int. J. quant. Chem., quant. Chem. Symp.*, **29**, 657.
PAPOUSEK, D., and ALIEV, M. R., 1984, *Molecular Vibrational–Rotational Spectra* (Amsterdam: Elsevier).
PARKER, G. A., ZHU, W., HUANG, Y., HOFFMAN, D. K., and KOURI, D. J., 1996, *Comput. Phys. Commun.*, **96**, 27.
PIMENTEL, G. C., and MCCLELLAN, A. L., 1960, *The Hydrogen Bond* (San Francisco, California: W. H. Freeman).
PINE, A. S., and LAFFERTY, W. J., 1983, *J. chem. Phys.*, **78**, 2154.
POPLE, J. A., BINKLEY, J. S., and SEEGER, R., 1976, *Int. J. quant. Chem., quant. Chem. Symp.*, **10**, 1.
POPLE, J. A., KRISHNAN, R., SCHLEGEL, H. B., and BINKLEY, J. S., 1979, *Int. J. quant. Chem., quant. Chem. Symp.*, **13**, 325.
PULAY, P., 1987, *Adv. chem. Phys.*, **69**, 241; 1990, *Program ANHAR* (Fayetteville, Arkansas: University of Arkansas).
PULAY, P., LEE, J. G., and BOGGS, J., 1983, *J. chem. Phys.*, **79**, 3382.
PURVIS, G. D., III, and BARTLETT, R. J., 1982, *J. chem. Phys.*, **76**, 1910.
QUACK, M., and SUHM, M. A., 1990, *Molec. Phys.*, **69**, 791; 1991, *J. chem. Phys.*, **95**, 28.
QUI, Y., ZHANG, J. Z. H., and BAČIC, Z., 1998, *J. chem. Phys.*, **108**, 4804.
RAGHAVACHARI, K., TRUCKS, G. W., POPLE, J. A., and HEAD-GORDON, M., 1989, *Chem. Phys. Lett.*, **157**, 479.
RÄSÄNEN, M., SEETULA, J., and KUNTTU, H., 1993, *J. chem. Phys.*, **98**, 3914.
REYNOLDS, P. J., CEPERLEY, D. M., ALDER, B. J., and LESTER, W. A., 1982, *J. chem. Phys.*, **77**, 5993.
ROSENSTOCK, M., ROSMUS, P., REINSCH, E. A., TREUTLER, O., CARTER, S., and HANDY, N. C., 1998, *Molec. Phys.*, **93**, 853.
SABO, D., BAČIC, Z., GRAF, S., and LEUTWYLER, S., 1998, *J. chem. Phys.*, **109**, 5404.
SCHLEGEL, H. B., 1982, *J. comput. Chem.*, **3**, 214; 1994, *Modern Electronic Structure Theory*, edited by D. Yarkony (Singapore: World Scientific), pp. 459–500.
SCHLEGEL, H. B., BINKLEY, J. S., and POPLE, J. A., 1984, *J. chem. Phys.*, **80**, 1979.
SCHMIDT, T. W., BACSKAY, G. B., and KABLE, S. H., 1998, *Chem. Phys. Lett.*, **292**, 80.
SCHWENKE, D. W., 1996, *J. phys. Chem.*, **100**, 2867, 18884.
SMITH, S. C., 1996, *Discuss. Faraday Soc.*, **102**, 17.
SPITZNAGEL, G. W., CLARK, T., CHANDRASEKHAR, J., and SCHLEYER, P. v. R., 1982, *J. comput. Chem.*, **3**, 363.
SUHM, M. A., and WATTS, R. O., 1991, *Phys. Rep.* **204**, 293.
SUN, H., and WATTS, R. O., 1990, *J. chem. Phys.*, **92**, 603.
SUTCLIFFE, B. T., and TENNYSON, J., 1991, *Int. J. quant. Chem.*, **29**, 183.
SZCZEPANIAK, K., CHABRIAR, P., PERSON, W. B., and DEL BENE, J. E., 1997, *J. molec. Struct.*, **436–437**, 367.
TENNYSON, J., 1992, *J. chem. Soc., Faraday Trans.*, **88**, 3271.
TENNYSON, J., and SUTCLIFFE, B. T., 1985, *Molec. Phys.*, **56**, 1175.

† Frequencies originally assigned to the neutral species have been reassigned to the ions by Milligan and Jacox (1970).

THOMPSON, K. C., JORDAN, M. J. T., and COLLINS, M. A., 1998, *J. chem. Phys.*, **108**, 564, 8302.
TRUHLAR, D. G., 1981, *Potential Energy Surfaces and Dynamics Calculations* (New York: Plenum).
URBAN, M., NOGA, J., COLE, S. J., and BARTLETT, R. J., 1985, *J. chem. Phys.*, **83**, 4041.
WALL, M. R., and NEUHAUSER, D., 1995, *J. chem. Phys.*, **102**, 8011.
WATTS, J. D., GAUSS, J., and BARTLETT, R. J., 1993, *J. chem. Phys.*, **98**, 8718.
WEI, H., and CARRINGTON, T., JR, 1992, *J. chem. Phys.*, **97**, 3029.
WILSON, E. B., JR, DECIUS, J. C., and CROSS, P. C., 1955, *Molecular Vibrations* (New York: McGraw-Hill); 1980, *Molecular Vibrations: The Theory of Infrared and Raman Vibrational Spectra* (New York: Dover Publications).
WOFFORD, B. A., BEVAN, J. W., OLSON, W. B., and LAFFERTY, W. J., 1986, *Chem. Phys. Lett.*, **124**, 579.
WOFFORD, B. A., ELIADES, M. E., LIEB, S. G., and BEVAN, J. W., 1987a, *J. chem. Phys.*, **87**, 5674.
WOFFORD, B. A., LIEB, S. G., and BEVAN, W. J., 1987b, *J. chem. Phys.*, **87**, 4478.
WOON, D. E., and DUNNING, T. H., JR, 1993, *J. chem. Phys.*, **98**, 1358.
WRIGHT, C. A., AULT, B. S., and ANDREWS, L., 1976, *J. chem. Phys.*, **65**, 1244.
WU, Q., ZHANG, D. H., and ZHANG, J. Z. H., 1995, *J. chem. Phys.*, **103**, 2548.
WYATT, R. E., 1995, *J. chem. Phys.*, **103**, 8433.
XANTHEAS, S. S., and DUNNING, T. H., JR, 1993, *J. chem. Phys.*, **99**, 8774; 1998, *Advances in Molecular Vibrations and Collision Dynamics*, Vol. 3, edited by Z. Bačić and J. M. Bowman (Greenwich, Connecticut: JAI Press), pp. 281–309.
YAMAGUCHI, Y., FRISCH, M., GAW, J., SCHAEFER, H. F., III, and BINKLEY, J. S., 1986, *J. chem. Phys.*, **84**, 2262.
YU, H.-G., and SMITH, S. C., 1997, *J. chem. Soc., Faraday Trans.*, **93**, 861.
ZHANG, D. H., and ZHANG, J. H. Z., 1995, *J. chem. Phys.*, **103**, 2548.
ZUNIGA, J., ALACID, M., BASTIDA, A., and REQUENA, A., 1996, *J. chem. Phys.*, **105**, 6099.